Physics – Uspekhi **38** (3) 287 – 317 (1995)

REVIEWS OF TOPICAL PROBLEMS PACS numbers: 42.11.+j; 47.27.–i; 47.32.–y

Hydrodynamics: problems and paradoxes

S K Betyaev

Contents

Dedicated to my teachers:
Professor Aleksandr Aleksandrovich Nikol'skii
and Vera Alekseevna Torzhkova

Abstract. This is a collection of topical hydrodynamic problems of different degrees of complexity, which are not ripe for mathematical modelling or for numerical calculations. Hints for obtaining solutions are given. Attention is concentrated on unexpected analogies between phenomena of different kinds and on establishment of new links between what are at first sight unrelated or isolated facts.

The feeling of mystery is the most beautiful feeling that man can experience. It is a source of any true art and science. One who has never experienced this feeling, who does not know what it is to stop and think seized in enthralling rapture, is like a dead man and his eyes are closed…
A Einstein

1. Introduction

In the last decades the interest in physics has shifted from field theory and from elementary particles to mechanics. Previously regarded as a fully complete branch of knowledge, mechanics has undergone profound changes. Gradually all new surprising properties of the evolution of dynamic systems have become clear and so has the decisive role of such antagonisms as stability – instability, randomness – regularity, continuity – discreteness, symmetry – asymmetry, evolution – revolution, and reversibility – irreversibility.

We can now speak of the establishment of a new science called synergetics which combines many branches of natural sciences ranging from astronomy to biology, and which largely relies on hydrodynamics (for the literature, see Ref. [1]). Convergence of sciences has led to a situation in which hydrodynamics is becoming part of synergetics. Only two divisions of hydrodynamics have become detached from the main body: they are physical and computational hydrodynamics. Physical hydrodynamics includes kinetics, flow of quantum liquids, relativistic hydrodynamics, and plasma dynamics.

Computational hydrodynamics has reached such a stage of development in its 40 years of existence that if a correct mathematical model is formulated, it is not difficult to find a method for its numerical verification [2 – 4]. Therefore, programming and calculation have become technical tools and autonomous topics, which now represent only the final stage of the mathematical modelling process represented by the triad: experiment – physical model – perturbation methods. Mathematical modelling or mathematical formulation of a problem should not be confused with computer modelling or simulation, which represents numerical calculation or simulation (involving the choice of an algorithm and programming).

S K Betyaev N E Zhukovskii Central Aerohydrodynamic Institute, 140160 Zhukovski-3, Moscow Province

Received 26 July 1993; revision received 15 November 1994
Uspekhi Fizicheskikh Nauk **165** (3) 299 – 330 (1995)
Translated by A Tybulewicz

The most powerful computers are being earmarked to tackle problems directly or indirectly related to hydrodynamics. For example, the IBM computer SP1 installed in 1993 at the Cornell University is intended to solve the problems in hydrodynamics, plasma physics, analysis of pollutants in air and ground water, development of new medicines, plotting ozone layer maps, and seismic analysis.

Although that part of unsolved problems which belongs to physical hydrodynamics is incomparably smaller than the remaining problems, the conclusion that fluid dynamics has become completely mathematical is unjustified. Hydrodynamics is a surprising science and the approaches following from it are effective in fields where at first sight the conditions are unsuitable for the application of the hypothesis of a fluid continuum. One example is that of particles and antiparticles. In spite of the still unfinished search for antimatter in the nearest stars, a hypothesis of cellular structure in the Galaxy has become popular: according to this hypothesis, matter is separated from antimatter by thin surface layers (known as the Leidenfrost layers) which are hot regions where matter is annihilated [5]. It is postulated that the radiation emerging from such layers is far too weak to be detected. How long does an antimeteorite fly before it burns up? How do matter and antimatter interact?

The problems can be divided into general and specific. Paraphrasing Planck's words on the physics of the nineteenth century and two unsolved problems (which were the finite velocity of light and the discrete nature of thermal radiation), we can say that hydrodynamics is almost complete and there are only two clouds on its bright horizon: Reynolds turbulence and separation of flow from a body. These are fundamental problems and their solution is of very great importance for further development of transport and power industries. These problems touch upon the content of the whole of theoretical hydrodynamics. The general problems are well known [6, 7] and there is no need to discuss them here.

The history of identifying specific unsolved problems in hydrodynamics began perhaps with Mark Twain when, well before the appearance of the theory of sound, he formulated the classical problem in acoustics: ''There ain't no way to find out why a snorer cannot hear himself snore''. Since then prominent mathematicians and physicists have made up collections of unsolved problems.

Soon after Hilbert formulated, at the turn of the century, his famous 23 problems, it became clear that they have not paved the road of progress in mathematics that has led subsequently to a revolutionary breakthrough in theoretical physics. Attempts to formulate the fundamental problems in physics have also suffered a fiasco because of unpredictability of the twists of imagination in science [8].

It is known that Einstein, who on top of everything else was also a designer and an inventor, was the author of the well-known problem of tea leaves [9]. Many famous scientists (Kolmogorov, Kapitza, Lavrent'ev, Sakharov [10–13] and others) have collected and published interesting unsolved problems. This paper deals with tens of unsolved problems in hydrodynamics [14].

The unsolved problems not only help in making science more systematic or act as a collection of paradoxes, but they also are a programme for action. Unsolved problems are identified most readily in mathematics because they can be formulated clearly as theorems. For example, the famous *Kourovka Notebooks*, published from 1962 onwards, contain about 800 such problems on the group theory and some of them have already been solved. In hydrodynamics, as in physics, the selection of unsolved problems is subjective and depends on the adopted scale of values, which makes it difficult to follow a systematic approach. For example, Fritz Ursell, professor at Manchester University, lists ten unsolved problems on the theory of waves [15].

Only one method, that of perturbation theory, is suitable for analytic solution of hydrodynamic problems. The development of the perturbation method and its applications are major recent achievements [16]. Numerical methods are something special. Their capabilities are extremely wide. Twenty problems in astrophysics, plasma physics, oceanology, turbulence theory, solid state physics, etc. are collected in Ref. [17].

Hydrodynamics, like any other branch of physics, can be divided into five parts:

(1) mathematical modelling of laminar flow;

(2) physical and mathematical modelling of turbulent flow;

(3) theory of flow separation;

(4) theory of stability;

(5) development of rheological models.

Problems which belong to all these parts are listed in Ref. [14].

Outstanding *solved* problems have usually appeared spontaneously. In hydrodynamics they are the following discoveries: (1) shock waves, by B Riemann (1860) and E Mach (1987); (2) chaos, by O Reynolds (1883); (3) the boundary layer, by L Prandtl (1904); (4) strange attractor, by E Lorenz (1963); (5) soliton, by M Kruskal and N Zabusky (1965); (6) fractals, by B Mandelbrot (1967); (7) catastrophes, by R Thom (1970). Not very rigorously, one should include here the development of synergetics by H Haken, professor at Stuttgart University (1977), and by I Prigogine, Nobel Prize Laureate.

Hydrodynamics is now unthinkable without the Fokker–Planck (Planck 1917), variational averaging (Whitham 1965), inverse scattering (Gardner et al. 1967) and renormalisation group (Wilson 1971) methods.

All these methods and discoveries, enriched with philosophical content, are now part of all natural sciences and not only of physics. These methods in conjunction with the perturbation theory concepts comprise what is now known as the *culture of hydrodynamics*.

There are dangers of reaching two extremal positions in selecting unsolved problems: one can become a fermatist or a provider of problems for doctoral theses. In contrast to a mathematician or a physicist, who can focus a narrow 'cone' of interests on the solution of just one problem, a hydrodynamicist has to master an extremely wide range of knowledge in his science and become an encyclopedist. This is in fact the meaning of the pithy saying: hydrodynamics is a humanist science.

The aim is not to obtain a solution, but to expose the problem. If somebody can predict in advance the results of a study, then that study is no longer a problem.

Those who hope to grasp the Navier–Stokes equation and use it in numerical calculations, so as to obtain results instantaneously, will be greatly disappointed. The path to the solution of a complex technical problem (such as the flow around turbine blades or an aircraft, flow in a wind

tunnel or in a chemical reactor, etc.) is difficult and involves many stages: the complete problem is split into several partial but no less difficult subproblems and if these are not solved the study straightaway becomes incorrect.

The collection of subproblems presented below is intended for inquisitive minds of whom Rene Descartes said: ''A curious person seeks rare events only to wonder at them, an inquisitive person seeks them in order to learn about them and cease wondering''.

The intermediate stage between the solved and unsolved problems is occupied by problems for which a mathematical model has been constructed and which await their turn for calculations. A contemporary collection of such problems, very interesting in their content, can be found in Ref. [18]. ''In exact sciences, as in art, beauty is the major source of light and clarity'' (W Heisenberg).

2. Construction of models

One of the sources for new formulations of problems is the improvement of the existing mathematical models. For example, the equation of motion of a mathematical pendulum, representing a material point at the end of a weightless string,

$$\frac{d^2x(t)}{dt^2} + x(t) = 0 , \tag{2.1}$$

where x is the angle by which the string is tilted from the vertical, can be 'improved' by a variety of methods. The range of validity of the mathematical model in terms of the values of $x(0)$ is widened slightly by inclusion of the following nonlinear term:

$$\frac{d^2x}{dt^2} + x - \frac{1}{6}x^3 = 0 . \tag{2.2}$$

A much more fundamental change to

$$\frac{d^2x}{dt^2} + \sin x = 0 \tag{2.3}$$

makes it possible to extend the range of validity of the above equation to all values of $x(0)$.

The mathematical model represents simplification of a real situation. Its validity depends on the targets which are set. For example, the oscillation period can be found from any one of Eqns (2.1)–(2.3). However, the number of oscillations until the pendulum stops cannot be found at all from these equations and one has to consider friction. In the linear approximation, we then have

$$\frac{d^2x}{dt^2} + k\,\frac{dx}{dt} + x = 0 . \tag{2.4}$$

The rolling and sliding friction in a joint is proportional, apart from the sign, to the load, i.e. $(dx/dt)^2$. When the values of $|dx/dt|$ are large, more exactly, when the Reynolds number Re is large, the aerodynamic resistance force is also large and proportional to the square of the velocity $(dx/dt)^2$. However, it is more correct to consider the coefficient k in Eqn (2.4) as dependent on $|dx/dt|$. But this model also does not correspond fully to reality.

A pendulum does not move in a medium at rest, but in a perturbed medium, i.e. in a wake. Therefore, a more rigorous model should take account of the memory, i.e. of the dependence on the prehistory of a process. This illustrates the transition from a simple oscillator to more complex unsolved problems in hydrodynamics. The specific mathematical model becomes more complex if a new hitherto ignored effect is included.

One can try to include stretching of the string, proportional to $(dx/dt)^2$, the weight of the string, etc., but one must recall here the familiar aphorism that ''any equation longer than 5 cm is most likely wrong''.

There are controlled and uncontrolled processes. If the strain (effect) l depends on the force (cause) F in such a way that $dl/dF = O(1)$, the process is controlled (Fig. 1a). If the derivative dl/dF is large, then the process is uncontrolled (Fig. 1b). Unsolved problems usually represent uncontrolled processes. The simplest familiar example of such a process is the growth of a tear in a newspaper sheet. When the force is applied to the edges of an initially formed tear (Fig. 2a), the process is controlled, but when the force is applied to the edges of the sheet (Fig. 2b), the process is uncontrolled.

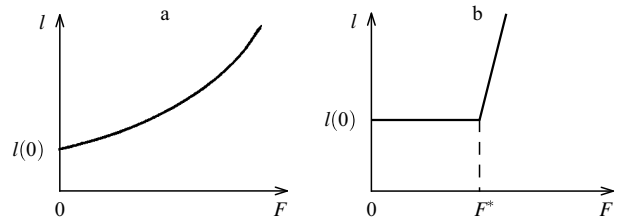

Figure 1. Controlled (a) and uncontrolled (b) processes.

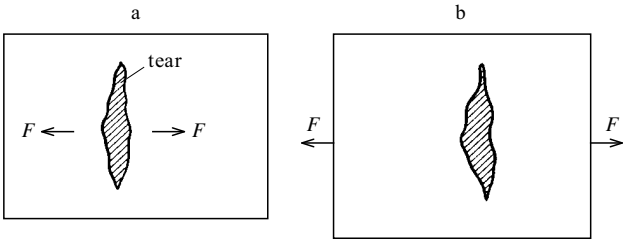

Figure 2. Evolution of a tear in a sheet of paper, showing examples of controlled (a) and uncontrolled (b) processes.

Hydrodynamics stands out from the whole of physics by the nonlinearity of its problems. Even the simplest approximations such as the model of an incompressible Newtonian fluid includes nonlinearities of the following types:

(1) convective — the term $(\boldsymbol{u}\cdot\nabla)\boldsymbol{u}$ in the Navier–Stokes equation governs the acceleration of a particle, ($\boldsymbol{u}$ is the particle velocity);

(2) rheological — the transport coefficients are functions of pressure and temperature;

(3) covariational, which represents the degree of correlation between the velocity of a fluid in different parts of space.

2.1 Modelling principles

Hydrodynamics is a science of modelling. The whole of its history, beginning from Helmholtz and even Newton, confirms this. There are three mutually related types of modelling: experimental, physical, and mathematical.

Experience is the foundation stone of any science, even as abstract as mathematics. The experiments of Faraday, Michelson, Hertz, and Mendel have been the seeds for such sciences as electrodynamics, theory of relativity, quantum mechanics, and genetics.

One can distinguish between several types of scientific experiments. If there is no hypothesis about the nature of the investigated phenomenon, then one would speak of an *exploratory* experiment. If there is a hypothesis, then an experiment is carried out in order to verify it and it can be called a *control* experiment. Finally, if there are several hypotheses, an experiment is performed to select one of them and it is called a *conclusive experiments*.

In addition to dividing experiments in accordance with their aim, in hydrodynamics one can divide them into *quantitative* and *qualitative*. Quantitative experiments yield numerical data, whereas qualitative experiments are used to determine the 'flow geometry', for example, the field of the paths of motion of fluid particles. The results of quantitative experiments are presented in the form of graphs or tables and those of qualitative experiments are illustrated by photographs or drawings. A quantitative experiment is usually of the 'black box' type: only the echo signal of a certain action on an object is recorded but the nature of the object remains unknown. Qualitative experiments are of great importance for hydrodynamics as a science.

The latter include what are known as '*experiments in a bath*'. They are unpretentious and inexpensive, and they can be carried out at home or in the physical laboratory of one's institute. As one prominent American experimentalist R Wood said, they can be done with a stick, string, sealing wax, and mica. However, the scientific importance of the experiments in a bath, which are represented extensively in this paper, is difficult to overestimate.

A collection of outstanding scientific experiments on fluid flow, which could be regarded as a catalogue of the gold treasure of hydrodynamics was made by Milton Van - Dyke, professor at Stanford University. He asked famous experimentalists all over the world to send photographs of the most interesting cases of flow. This enabled him to publish, in 1982, *An Album of Fluid Motions* [19], a masterpiece of both scientific and popular literature on hydrodynamics.

Industrial experiments are more widely known than scientific ones. They are carried out in wind tunnels, on benches, in tanks, and in channels at the request of a design department. Usually industrial experiments are quantitative and their aim is to establish the optimal shape of an aircraft, a rocket, a ship, or a turbine blade.

A mathematical model is based on a physical model (deduced from first principles of physics) and a qualitative experiment. The simplest structure of scientific and technical relationships in hydrodynamics is shown schematically in Fig. 3. The link between qualitative experiment and mathematical model represents the transition from contemplation to scientific understanding of a phenomenon. Construction of a mathematical model represents the strategy of a numerical calculation, but not its performance [20].

Like the theory of relativity, the theory of mathematical modelling is the cutting edge of philosophical problems in hydrodynamics and can be divided into general and special. Rheological models of a non-Newtonian fluid are developed on the basis of the general theory. The special theory deals with continuous Newtonian media. Under the

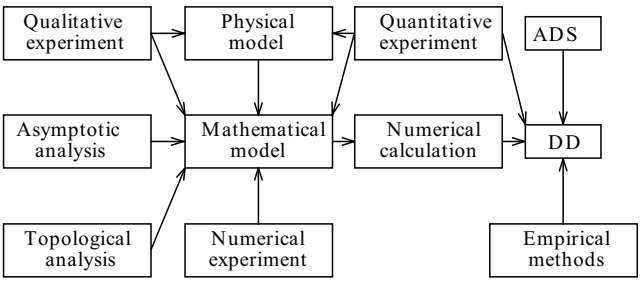

Figure 3. Structure of scientific and technical relationships. Here, ADS is an automated design system and DD is a design department or bureau.

conditions not very different from those on the Earth, i.e. those dealing with the practical requirements of aircraft construction and shipbuilding, the flow of a continuous medium obeys the Navier–Stokes (NS) equation. In the case of an incompressible fluid which is not subject any external forces, this equation is

$$\frac{\mathrm{d}\boldsymbol{u}}{\mathrm{d}t} = -\frac{1}{\rho}\nabla p + \nu\nabla^2\boldsymbol{u}, \qquad \nabla\cdot\boldsymbol{u} = 0\,, \tag{2.5}$$

where p is the pressure, ρ is the density, ν is the kinematic viscosity, and t is time.

The Euler (E) equation is obtained if we assume formally $\nu = 0$. When the NS equation is converted to its canonic form, we go over from physical to mathematical modelling and we meet immediately the familiar difficulties: the solution of the NS equation cannot be obtained for sufficiently large Reynolds numbers Re and the E equation has an infinite set of solutions, whereas the Prandtl boundary-layer equation does not always have a solution.

In the limiting case when the Reynolds number $Re = u_\infty l/\nu$ (u_∞ is the velocity of homogeneous free-stream flow and l is a typical dimension of the body in the stream) is small, the NS equation reduces to the Stokes (S) equation. In the other limiting case when $Re \gg 1$, the NS equation reduces to the E equation. The reality is not as simple: there is a large number of differential, integral, and integro-differential equations which correspond to asymptotic submodels of hydrodynamic phenomena. Fig. 4 shows only some of these equations. The designations used in this figure are as follows: P stands for the Prandtl boundary-layer equations, $\overline{\mathrm{NS}}$ are the averaged NS equations, NS′ are the reduced (parabolised, hyperbolised, etc.) NS equations, AT are the asymptotic theory equations (linearised NS equations, equations of interaction, equations of marginal separation, etc.), L is used for the Laplace equations, L(D) is the Laplace equation with discontinuities (slip surfaces), EVS, ECD, and EFS are integrodifferential equations for the evolution of a vortex sheet, of a contact discontinuity, and of a free surface.

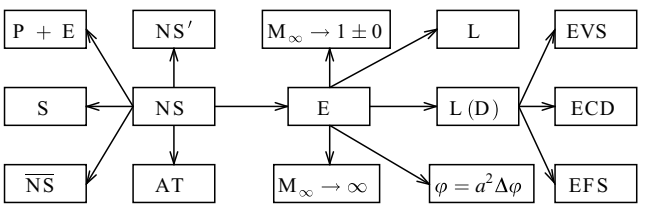

Figure 4. Equations of fluid dynamics (explanations in text).

The points, lines, and surfaces on which the solution is not smooth are called *folds*. It is particularly important to monitor the correctness of a mathematical model in the vicinity of folds where the nonlinearity is 'concentrated'. A correct mathematical model should have local asymptotic expansions near all the folds.

Unfortunately, these expansions are not always known. This is, in particular, the reason why various empirical principles are used widely in hydrodynamics. The *principles of indeterminacy* prohibits the use of deterministic calculation methods in regions where the flow is chaotic; this principle justifies introduction of such 'fuzzy' notions as separation, turbulence, etc. The *principle of maximal simplicity* postulates the minimum number of separations on a smooth surface, boundedness of the solution (the Kutta and Brillouin–Villat conditions) and the minimal singularity in the solution of the problem by the method of deformed coordinates (the Lighthill rule). The p*rinciple of convergence* implies that both experiments and numerical calculations are repeatable and reproducible. The *principle of forbiddenness* imposes familiar physical limits from above and below on hydrodynamic quantities and on the space–time scale of flow; for example, the concept of a continuous medium, i.e. the NS equation, breaks down at distances of the order of $O(Re^{-1})$ and after time intervals $O(\tau)$, where τ is the mean free time. The *principle of extremal correspondence* implies that a mathematical model should be reduced to a known model for the limiting values of the parameters 0, 1, or ∞; this can be used as a criterion in selection of models suitable in practice and its effectiveness has been demonstrated in the selection of quantum-mechanical theories.

2.2 Perturbation methods

Asymptotic analysis of the correctness of a mathematical model is based on perturbation methods suitable for the solution of the equation $f(x; \varepsilon) = 0$ when the parameter ε can be regarded as small ($\varepsilon \to 0$) or large ($\varepsilon \to \infty$). One case goes over to the other by, for example, the substitution $\delta = 1/\varepsilon$.

Perturbation methods are the foundations of any theory (those of Euclid, Newton, Darwin, Smith, Marx, Einstein, Vernadskii, etc.) because each of them represents idealisation of an actual phenomenon, proposed on the assumption that some of the determining parameters go to their limiting values ($\varepsilon = 0$). Perturbation methods are not a tribute to fashion and they do not represent abstract mathematical apparatus, but they are the tools of a natural scientist. They have the dominant position both in fundamental research and in applications, and they compete quite successfully with calculation methods.

The correctness of perturbation methods, which first appeared at the beginning of the nineteenth century, has never been proved. This is the drama of ideas: physicists employ methods which are not accepted by 'pure' mathematicians (purists).

Perturbation methods were not the result of a sudden discovery of one mathematician. Among the many scientists who worked on these methods one should mention three prominent contributors.

The French astronomer, mathematician, and physicist Pierre Simon Laplace (1749–1827) used extensively series in his work. He solved the problem of equilibrium of a large weightless drop on a plane and he was the first to use perturbation methods. This was an intuitive breakthrough into the unknown. Laplace gave an amazingly rich description of perturbation methods: ''a mathematical method is the more precise the greater is the need for it''.

The French mathematician Augustin Louis Cauchy (1789–1857), one of the founders of mathematical analysis, proposed a clear theory of convergent series indicating the criteria for their convergence. Naturally, divergent series were at that time of no interest to Cauchy. His authority was so great that practical applications of asymptotic expansions were delayed for a long time. At present the asymptotic (and as a rule) divergent series are an important investigative tool.

The idea of deformed coordinates dates back to the outstanding French mathematician Jules Henri Poincare (1854–1912). He obtained a uniformly applicable asymptotic expansion by altering slightly the coordinate x and also by expanding it as an asymptotic series. Thus, together with an expansion for an independent variable,

$$f(x; \varepsilon) = f_0(s) + \varepsilon f_1(s) + \varepsilon^2 f_2(s) + \dots ,$$

he constructed a series for the coordinate

$$x(s; \varepsilon) = s + \varepsilon x_1(s) + \varepsilon^2 x_2(s) + \dots ,$$

where s is a new coordinate replacing x. The functions $x_n(s)$ representing the deformation of the coordinate x, are not a priori known and have to be found successively in the course of solution of the problem.

The history of perturbation methods is marked by two triumphal moments.

In 1846 the French astronomer, a Foreign Corresponding Member of the St Petersburg Academy of Sciences, Urbain Leverrier discovered a planet, later called Neptune. The discovery was unusual: Leverrier did not use a telescope, as was done always by his predecessors in similar discoveries. He found a new planet 'at the tip of a pen' by investigating *perturbations* which this mysterious invisible object caused in the motion of another planet — Uranus. In the same year 1846 the coordinates calculated by Leverrier were used by the German astronomer Johann - Galle to discover (with a telescope!) the hitherto unknown planet.

This was the first triumph of perturbation methods. The second was the discovery in 1905 (once again 'at the tip of a pen'!) by the prominent German hydrodynamicist Ludwig Prandtl (1875–1953) of what we know as the boundary layer — a thin region adjoining the surface where the velocity of flow of a low-viscosity fluid changes very rapidly. This discovery was of very great importance for the subsequent development of the transport and power industries.

Today not only physicists, but also mathematicians denote by boundary layer a narrow region or a small interval where a function undergoes rapid changes.

Many perturbation methods have been developed: they include the method of matching asymptotic expansions, the method of multiple scales, the method of deformed coordinates, etc. There are so many of them that physicists joke that ''there are as many perturbation methods as there are problems''.

Among all the possible perturbation methods the first place in hydrodynamics is occupied by the method of matching asymptotic expansions, which has changed from a purely mathematical tool to a category of physical thinking. The method of matching asymptotic expansions is

effective when there are at least two different, in order of magnitude, scale lengths which define two regions: outer and inner, and in each of them a specific asymptotic expansion is valid.

Imagine that you have a photograph (outer region) with an unclear but important detail, which because of its small size looks like a singular point (inner region). If this region is viewed with a magnifying glass, i.e. under multiple magnification (stretching of coordinates), then somewhere at its periphery we can see the details which are hardly distinguishable in the vicinity of this singular point in the unenlarged photograph. This is the essence of the method of matching asymptotic expansions.

2.3 The Prandtl paradigm

The limit $Re \to \infty$ is special. Prandtl's concept of a boundary layer, valid for nonseparated flow past a body, can be generalised in a natural manner to separated flow. Fig. 5 shows schematically the pattern of limiting flow past a schematic body with a spike. There are three characteristic regions: (1) thin viscous layers where the P equations are valid (1A are boundary layers; 1B are mixing layers; 1C is a wake); (2) vicinities of folds, where the P and E equations are not valid and a more careful application of the NS equation is necessary (2A and 2B are the vicinities of the lines of separation from a smooth surface and of a corner edge; 2C and 2D are the vicinities of a line of reattachment to a smooth surface and to a corner edge; 2E is the vicinity of the tip of a cavity or a closed circulation zone; 2F is the vicinity of a spiral core of a tangential discontinuity, a line where discontinuities cross, etc.); (3) a region of ideal fluid flow (3A is a region of vortex-free flow; 3B is a region of vortex flow). Since in the limit $Re \to \infty$ the thicknesses of regions 1 (where small amounts of mass, momentum, and energy are concentrated) and the dimensions of local zones 2 vanish, it follows that the boundary layers become coincident with the surface of a body and the mixing layers contract into vortex surfaces of discontinuity of the tangential component of the velocity. Therefore, in a certain range of scales, which are not too small, so as not to include viscous layers, and not too large, so that the diffusion of the wake is still unimportant (for example, on the scale of the body which is considered here), the flow corresponding to the limit $Re \to \infty$ can be regarded as inviscid. The E equations apply in regions 3. Flow subregions are separated by tangential discontinuity surfaces: a *contact discontinuity*, which separates liquids with different densities and which appear in media consisting of two or more phases; a *vortex sheet*, separating parts of the same liquid (which is a special case of a contact discontinuity); a *free surface*, separating a region of flow from a region at the boundary of which the pressure is assumed to be given. At a contact discontinuity we have zero flow velocity on both sides and the pressure jump is equal to the effective pressure representing the action of the surface tension forces. The pressure is continuous across a vortex sheet. On a free boundary the flow velocity is zero on the moving fluid side and also there is a given pressure which is generally a function of the surface coordinates and time. In a special case a free surface is a boundary of an isobaric region. Surface forces may act on a free boundary.

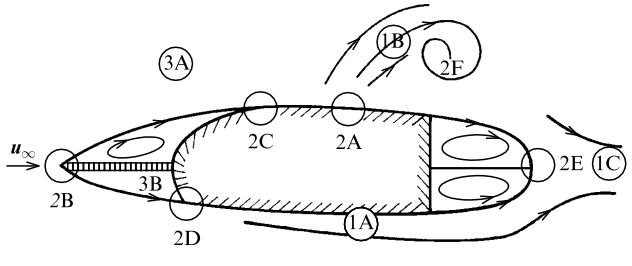

Figure 5. Pattern of flow of a low-viscosity fluid past a schematic body.

A vortex sheet and a free boundary are defined for a compressible fluid also as surfaces of discontinuity of the tangential component of the velocity. The density of a gas has a discontinuity at a vortex sheet.

The solution of the E equation is piecewise analytic: parts of space are separated by piecewise analytic surfaces of discontinuity of the velocity (slip surfaces, weak discontinuities, and shock waves) and functions or their derivatives suffer a jump of the first kind when they cross these surfaces. Folds are those lines on which the surfaces of discontinuity are nonanalytic. The folds form as intersections of discontinuity surfaces with one another and with the body past which the flow occurs. In their turn, the folds are also piecewise analytic. The points at which they are nonanalytic are singularities. The folds and the singularities may appear, merge, or escape to infinity as time passes. It is not yet clear which singularities of functions and surfaces can exist at the folds. These questions are being investigated by coordinate expansions within the framework of the E equation, and by the methods of matching asymptotic expansions on the basis of the NS equation. There is a close relationship between these two theories: the internal limit of an expansion in the theory of flow of an ideal fluid is equal to the external limit of an expansion in the theory of a viscous fluid.

2.4 Hierarchy of models

Three main requirements have to be satisfied by a mathematical model: it must agree with experiments, it must also agree with the initial physical model, and the problem must be well-posed. Apart for a qualitative similarity between the mathematical model and the flow patterns observed in wind and water tunnels, a quantitative agreement is necessary (within the limits of a certain error) between the calculated and real characteristics: the model must satisfy practical requirements. At present, the demand that a problem be well-posed is much weakened by the absence of suitable theorems. It is postulated that a (piecewise analytic) solution does exist. The solution need not be unique, since this can be checked experimentally, and it need not be correctly posed in the Hadamard sense.

It would seem that when the full problem of flow past a body is split into a number of auxiliary problems in accordance with the $\mathrm{NS} \to \mathrm{E} + \mathrm{P} + \mathrm{NS}'$ scheme, we can solve the E equation and thus find the boundary conditions for the P equation, which can then be solved, and the solution can be considered in specific regions on the basis of the reduced NS' equations. However, this simplistic programme would fail: a model of an ideal fluid ('dry water' model) is not logically closed. The difficulty is as follows: in the course of formal passing to the limit $Re \to \infty$ the higher

derivative is lost from the NS equation and this means the loss of information about flow: about smoothness, uniqueness, asymptotic behaviour at large distances or after a long time, and sometimes even about the existence of a solution. The 'dry water' model does not have a unique solution even when it is supplemented by reasonable conditions (the Kutta conditions that the pressure should be finite at the corner edge of a body in a flowing fluid, the Brillouin – Villat condition that the pressure gradient should be finite on the line of separation of a tangential discontinuity surface from the smooth surface of a body, and the Batchelor condition, which represents an equation for determination of the vorticity in a closed circulation region). We thus find that in the 'dry water' model we cannot obtain a unique solution a priori, because without diagnosis of the boundary layer the positions and numbers of points of separation, i.e. of slip surfaces starting at a body, remain unknown. The two problems, i.e. the solution of the E and P equations, are so closely related that the formal (though correct from the point of view of the perturbation method) separation of them has to be empirical. The solution of the E equation requires additional assumptions about the number and sometimes also about the shape of the discontinuity surfaces, and also about the presence of closed vortex zones adjoining the surface of a body in a flowing fluid.

However, separation of the problem results in a fundamental simplification: turbulence typical of low-viscosity flow is concentrated in thin layers. In hydrodynamics a stochastic layer coincides with a boundary layer and a mixing layer [21]. This is the physical reason for the instability of discontinuity surfaces. In the absence of stabilising factors the slip planes have a Helmholtz instability or, in other words, a Lyapunov instability. The 'instability in the small' changes the 'dry water' flow pattern if the frequency of fluctuations is high or if their amplitude reaches finite values. The thin viscous layer concept becomes invalid even earlier, when the amplitude of displacements of a discontinuity becomes of the same order of magnitude as the thickness of a mixing layer.

Essentially ill-posed and conditionally ill-posed problems are very different from the mathematical point of view. The absence of a solution of an ill-posed problem is evidence that the model is not selected correctly and that the problem has to be reformulated. However, this classification is speculative until a criterion is found how to distinguish between these two types of ill-posed problems.

A specific model can be improved by introducing a new effect ignored at the preceding stage. The most striking example of such an improvement is the hierarchical series of mathematical models used in the theory of a low-aspect-ratio wing, known as a small-elongation wing in Russian terminology, where elongation is a parameter that determines the extent of the wing in the direction of free-stream flow [22]. A model without flow separation (Fig. 6a; here and later the cross sections of a wing are shown) leads to infinite velocities at the wing edges ($y = 0$, $z = \pm 1$), since the Kutta condition is not satisfied. The Legendre model (Fig. 6b) resolves this conflict, but it leads to an ambiguous solution because of a pressure discontinuity on the AF line which joins a point vortex at a point F to the wing edge A [23]. The 'vortex – cut' scheme (Fig. 6c) avoids this ambiguity, but there is then an indeterminacy in respect of the shape of AF [24]. A separation model with spiral vortex

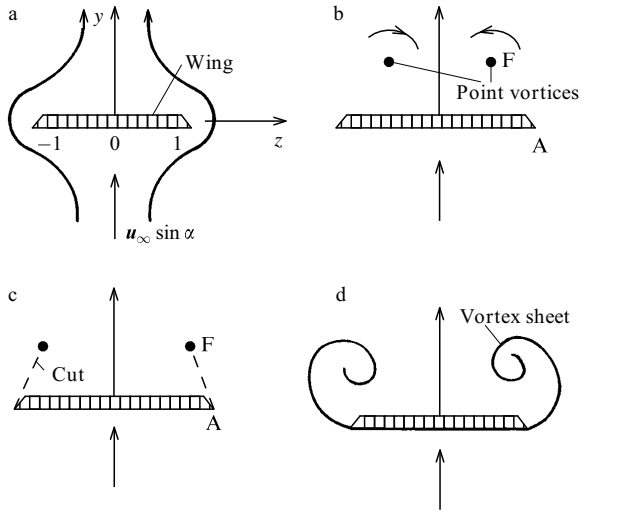

Figure 6. Patterns of flow past a low-aspect-ratio wing, deduced on the basis of nonstationary flow analogy.

sheets starting at the edges [25] is free of this indeterminacy (Fig. 6d) but it predicts an infinite pressure gradient on approach to the edge along the top surface of the wing.

Numerical experiments, which represent the 'head-on' solution of the E or NS equations, occupy a special place in the hierarchy of methods used to solve hydrodynamic problems. In the pre-computer era such numerical experiments were pioneered by giants such as Masau [26], Rosenhead [27], Westwater [28], Kaden [29], and Fermi [30]. Numerical experiments should be considered not only as a means for obtaining quantitative results, but also of determining whether the problem is well-posed. Such 'brute force' methods can only give qualitative results. The range of applications of numerical experiments in hydrodynamics has shrunk under the influence of our expanding knowledge of the properties of flow of low-viscosity fluids.

2.5 Paradoxes

A paradox is an unexpected conclusion that is in stark contrast to what is generally accepted. The practical value of paradoxes, which are the driving engines of progress, is that they force one to take a fresh look at the foundations of an older theory and to develop a new improved theory and sometimes a new science. The special theory of relativity represents the resolution of the paradox of the finite rate of information transfer and quantum mechanics is a resolution of the paradox of discontinuity of signals in the microscopic world. Paradoxes have given rise to the physics of elementary particles and to modern cosmology, and have stimulated the development of modern mathematics.

''The facts that we come up against seem at first completely paradoxical from the mathematical point of view, an can only be examined on the basis of purely physical considerations'' (J Hadamard).

If we can distinguish a tentative judgement based on experiments from a theoretical one based on mathematical modelling of a phenomenon, we can classify paradoxes into three types.

First, there are the conflicts between the generally accepted and new theoretical propositions. These are perhaps the simplest paradoxes (of the 'theory – theory' type) and they arise as a result of improvement of a

mathematical model and calculation methods. The paradoxes of nonunique solutions and of infinity are among them.

The second type of paradox involves a conflict between what is generally accepted and new experimental evidence ('experience – experience'). Examples of such paradoxes are those that concern symmetry. Symmetry breaking or appearance, considered from the point of view of synergetics, is a transition to a different (stable) level of organisation which occurs under the action of all small asymmetric perturbations present in flow. This is, of course, a far too general explanation and each specific problem requires a detailed analysis. Another example is the Eiffel paradox: the drag of a sphere decreases abruptly (by a factor of 4 – 5!) with increase in the velocity near the 'critical' Reynolds number, which is approximately 150 000. This observation, which is in conflict with our expectations, is also associated with a transition of flow to a different level of self-organisation, namely from laminar to turbulent flow.

Paradoxes of the third type ('theory – experience' or 'experience – theory') are characterised by a conflict between the theoretical results and what we call experience, intuition, or simply common sense. The most famous of the paradoxes of this type is the Euler – d'Alembert paradox of zero resistance of a body moving in a frictionless fluid. It can be regarded as one of the symmetry paradoxes: if the flow well ahead of a body is the same as far behind it, it follows from the law of conservation of momentum that the resistance force vanishes. In real flow (in accordance with our experience) the symmetry is always broken: a wake forms behind a body and it represents a stagnant 'stream' of a fluid.

Contemplation is a primitive form of cognition, whereas identification of contradictions of paradoxes is a complex gnosiological process. Everyone facing a discrepancy asks the question ''Why?'' ''Why does an apple fall down?'' was the question asked by Newton and the answer was the law of universal gravity.

Unresolved problems are unsolved paradoxes. Unlike solved paradoxes, which are now part of history, the unsolved ones still excite the minds of scientists. A paradox is what is born as a paradox but dies of banality.

3. Self-similar flow

'Self-similarity' is called 'auto-modelling' in Russian. The Russian phrase is poorly made up. The first part, 'auto', though of foreign origin, does reflect correctly the nature of the phenomenon, whereas the second part is completely out of place. It is better to follow the English terminology and speak of 'self-similarity'. Unfortunately, 'auto-modelling' is now customary in Russian and it would be impossible (rather than difficult) to alter it.

Self-similar flow is virtually an intermediate asymptote of real flow [31 – 33]. One can say that real flow attains the self-similar regime in a certain space – time interval only in the sense that real flow is described by the self-similar approximation subject to a certain error. The influence of non-self-similar factors (counterpressure, asymmetry, viscosity, other real properties of a gas, etc.) is important over short and long times and particularly near singularities of flow and at infinity. If the background of non-self-similar factors is small, the hypothesis of self-similar flow is on the whole valid, subject to the additional assumption that the flow is laminar, but this has to be checked experimentally.

Self-similar solutions are exceptionally important because they are almost the only type of initial data in the Cauchy problem describing evolutionary processes in the dynamics of liquids and gases. For example, at the moment of appearance of discontinuous flow the number of determining parameters is minimised and this means that the hypothesis of self-similarity can be used. The existence of a self-similar solution is crucial for the existence of solutions of complete non-self-similar problems, which can be obtained readily by numerical methods under the familiar conditions of the Cauchy – Kovalevskaya theorem.

Self-similarity implies that in the four-dimensional space $\boldsymbol{r}_1, t$ there are quasiconical coordinates $\boldsymbol{r} = \boldsymbol{r}_1/bt^n, t$ $(0 \leqslant t \leqslant \infty)$ and that the dependence on t is expressed in an explicit (power law) form. The vector $\boldsymbol{r}$ describes the velocity of motion of a point under consideration. Therefore, the relative velocity vector $w = \boldsymbol{u} - \boldsymbol{r}$ becomes important; here,

$$n\boldsymbol{u}(\boldsymbol{r}) = \frac{\boldsymbol{u}_1(\boldsymbol{r}_1, t)}{bt^{n-1}} ,$$

where $\boldsymbol{u}_1$ is the viscosity vector of particles in a liquid. Therefore, the Euler equations for a compressible gas are found to be elliptic in the range where $|w|^2 < a^2 = \gamma p/\rho$ (γ is the adiabatic exponent of a perfect gas and a is the velocity of sound) and hyperbolic in the range where $|w| > a$.

The parametric family of the vector lines $w \times \mathrm{d}\boldsymbol{r} = 0$ defines a field of self-similar paths. Let us now consider how these lines are selected for the same fluid particles at the initial moment $t = 0$. If we adopt physical variables, we find in the limit $t \to 0$ that

$$(t\boldsymbol{u}_1 - n\boldsymbol{r}_1) \times \mathrm{d}\boldsymbol{r}_1 = \boldsymbol{r}_1 \times \mathrm{d}\boldsymbol{r}_1 = 0 .$$

It therefore follows that each self-similar path is initially a straight line passing through the origin of the coordinate system. The field of self-similar paths is not solenoidal, $\nabla \cdot w = -2$, even in the case of flow of an incompressible fluid.

The topological properties of self-similar flow are determined by the nature and positions of singularities of a field of self-similar paths defined by $w = 0$. There are numerous types of singularities. A singularity of the 'focus' type occurs at the core of spiral discontinuity or in the vicinity of a point vortex, and its presence indicates that the flow has separated. Singularities of the 'centre' type cannot appear in flow if there are no fluid sources, whereas a singularity of the 'node' type is associated with self-similar paths even in the absence of sources, because a field of such paths is not solenoidal. If linearisation in the vicinity of a singularity is invalid, more complex types of singularities appear, for example, a saddle + node singularity. Such a situation occurs when singularities merge and the parameters reach their critical values. All the singularities are located in a region where equations of the elliptic type are valid or on the boundary of this region, which is a parabolic surface.

3.1 Classification

Let us assume that unsteady flow of a perfect gas or an incompressible liquid is governed by two parameters ρ_0 and b with independent dimensions:

$$[\rho_0] = ML^{-3}T^{-kn}, \quad [b] = LT^{-n}.$$

The self-similarity index n is characteristic of the law of expansion or contraction of a flow region. The exponent k vanishes for an incompressible fluid.

First, we have to identify the time interval $t_1 \leqslant t \leqslant t_2$ where a self-similar solution exists. Two forms of self-similar flow can be distinguished [34]. If this flow has appeared 'recently', i.e. if $t_1 = O(t)$, it follows from the invariance of the solution with respect to a time shift that we can always assume $t_1 = 0$ and that a self-similar solution exists for positive times ($t_2 = \infty$). If this flow has started 'long ago', i.e. if $t_1 = -\infty$, a self-similar solution exists for negative times: $-\infty < t < 0\,(t_2 = 0)$.

The influence of non-self-similar factors responsible for the appearance of self-similar flow is important at the initial moment $t = t_1$. The influence of non-self-similar factors responsible for suppression of self-similar flow is important at the final moment $t = t_2$. The question of the role of these factors is usually resolved a priori from considerations of the dimensions.

Let us consider this in detail by taking as our example the viscosity force acting in a Newtonian liquid with a constant kinematic viscosity v. The influence of this factor can be described by the Reynolds number

$$Re = \frac{u_\infty l}{v} = O\left[(\pm t)^{2n-1}\right]$$

where u_∞ and l are the velocity and length scales, and the upper or lower sign is selected for the positive and negative time intervals, respectively. Such flow is strictly self-similar if $n = \frac{1}{2}$ (Birkhoff flow [35]). If $n \neq \frac{1}{2}$, we can only speak of the motion of an ideal gas, i.e. of a self-similar solution of the E equation. However, will the influence of the viscosity force be so low or localised that the flow as a whole can be regarded as inviscid? This central problem in hydrodynamics of low viscosity fluids has not been resolved in general.

If the Reynolds number Re decreases with time from infinity to zero, there must come a moment when the influence of the viscosity force becomes the dominant one. Therefore, a necessary condition for the existence of a self-similar solution in the case when $n \neq \frac{1}{2}$ is an increase in Re with time from zero to infinity, i.e. the condition $Re(t_1) = 0$. Consequently, the solution is physically real† in the half-interval $0 < t < \infty$ if $n > \frac{1}{2}$, and it is also real in the interval $-\infty < t < 0$ if $n < \frac{1}{2}$. The full circulation of each vortex zone of physically real flow increases from zero to infinity, like the Reynolds number Re.

If we begin with the condition of physical reality of self-similar flow, we can immediately reject the possibility that the solution on the semiaxis $o < t < \infty$ can be continued to negative values t. In contrast, the solution in the interval $-\infty < t < 0$ sets the initial conditions at $t = 0$ for continuation of this solution to positive values of t. If such a continuation exists, it follows form the consideration of the dimensions that it should have the same self-similarity index as the initial solution and that this is lost with time under the influence of the viscosity force.

The solution of the semiaxis $-\infty < t < 0$ describes collapse (a contact discontinuity, a free boundary, or a shock wave) if $n > 0$ and it corresponds to expansion if $n < 0$.

Whole classes of self-similar flow are known in hydrodynamics of an ideal fluid and they are listed below.

(1) Incompressible fluid. The self-similarity index is arbitrary. It is possible to distinguish [34] pseudosteady flow ($n = 0$), Birkhoff flow ($n = \frac{1}{2}$), Kaden flow ($n = \frac{2}{3}$), exponential self-similar flow ($n \to \pm\infty$), and unsteady conical flow ($n \to \pm 100$). A one-dimensional example is symmetric collapse of a cavity.

(2) Compressible fluid. The presence of a dimensional parameter, which is the velocity of sound in free-stream flow, determines the unique value of the self-similarity index, which is unity. Each fixed point in a self-similar plane moves at a constant velocity; a coordinate system linked to the moving surface is inertial; the quantity b has the dimensions of velocity; the pressure of an unperturbed gas, which is of constant density, can be taken into account within the framework of the self-similarity hypothesis. One of the determining parameters is the Mach number M_∞ for free-stream flow. One-dimensional examples are decay of an arbitrary discontinuity and the motion of a flat piston.

(3) Hypersonic flow. The self-similarity index is arbitrary again. It is postulated that in nonuniform ($n \neq 1$) free-stream flow the velocity of sound a_0 is negligible compared with the velocity of a shock wave. Therefore, only compressive flow with a strong shock wave ($M_\infty = \infty$) is possible. The model defined in a positive time interval is self-similar for $t \gg t_0$ in the case of accelerated flow ($n > 1$) and for $t \ll t_0$ in the case of retarded flow ($n < 1$); here, $t_0(a_0/b)^{1/(n-1)}$, $0 < t < \infty$.

Accelerated self-similar flow of a gas is preceded by an acoustic stage of evolution of weak discontinuities for $t \ll t_0$ and by a transition stage of formation of hypersonic flow when $t = O(t_0)$. An 'entropy layer' of a stagnant gas with the characteristic thickness bt^n forms at the transition stage.

One-dimensional examples of a hypersonic self-similar flow are the motion of a piston, a strong explosion, and collapse of a shock wave.

(4) Conical flow is an example of steady self-similarity [23, 36]. The solution is independent of the linear coordinate, but it depends only on two angular coordinates. The problem is then two-dimensional. A one-dimensional example is the flow past a circular cone oriented at zero angle of attack.

In hydrodynamics of a Newtonian fluid the self-similarity index of flow of an incompressible fluid is, as mentioned before, $\frac{1}{2}$ for the complete NS equations. A steady self-similar flow can be represented as follows in a spherical system of coordinates r, θ, λ:

$$\boldsymbol{u}(r, \theta, \lambda) = \frac{v}{r}\boldsymbol{U}(\theta, \lambda), \quad p(r, \theta, \lambda) = \frac{v^2}{r^2}P(\theta, \lambda).$$

In a nonideal medium with a constant Prandtl number Pr and with its kinematic viscosity depending on temperature in accordance with the power law ($v = aT^k$) the self-similarity index is fixed:

$$n = \frac{1 - 2k}{2 - 2k}, \tag{3.1}$$

†The term 'physically unreal' or meaningless is not the same as in mathematics. The existence of a physically unreal solution can only stimulate an investigator to broaden the formulation of the problem.

and the steady self-similar solution becomes

$$\boldsymbol{u}(r,\,\theta,\,\lambda) = b^{\alpha} r^{m} \boldsymbol{U}(\theta,\,\lambda)\,, \qquad p(r,\,\theta,\,\lambda) = b^{2\alpha} r^{2m} P(\theta,\,\lambda)\,,$$

where $b = a\mathcal{R}^{-k}$, $\alpha = 1/(1-2k)$, $m = 1 - 1/n$, and $\mathcal{R}$ is the gas constant.

3.2 Ideal fluid

Nikol'skii [37, 38] was the first to investigate the solution describing the motion of a point vortex of strength Γ_0 or several points vortices, which is physically meaningful in the case of unsteady self-similar flow when the flow-similarity index n approaches $\frac{1}{2} + 0$. This solution is applicable to the flow past an infinite wedge (Fig. 7a) and flow past a finite body (plate, Fig. 7b), which is considered in Ref. [39]. The Nikol'skii flow is characterised by an increase in all the dimensions of the body and the path travelled by it proportionally to $\sqrt{t}$. This type of flow includes that inside a wedge at a constant rate (Fig. 7c).

The Nikol'skii theory can be applied to separated flow if certain quantities are selected a priori, for example the number of point vortices which simulate a vortex that has become separated from the investigated body. The situation is suitable for modelling separation of flow from a wedge-shaped edge of a body when the problem satisfies additionally the Kutta condition.

The Nikol'skii flow represents a special case of the Birkhoff flow ($Re = \infty$). Some examples of the Nikol'skii flow, which can be used to study the existence, bifurcation, topology, and asymmetry of self-similar solutions can be found in Ref. [14].

One of the surprising phenomena which occur in a system of three or more point vortices is collapse, which is essentially the Nikol'skii flow in a rotating coordinate system [40]. Vortices with complex coordinates $z_j(t)$ travel along spiral paths to a point where they collapse after a finite time (Fig. 7d).

Consider a cluster of three vortices which evolve in accordance with the law

$$\frac{\mathrm{d}\overline{z_j}(t)}{\mathrm{d}t} = \frac{1}{2\pi\mathrm{i}} \sum_{k \neq j} \frac{\Gamma_k}{z_j - z_k}\,, \qquad j = 1, 2, 3\,,$$

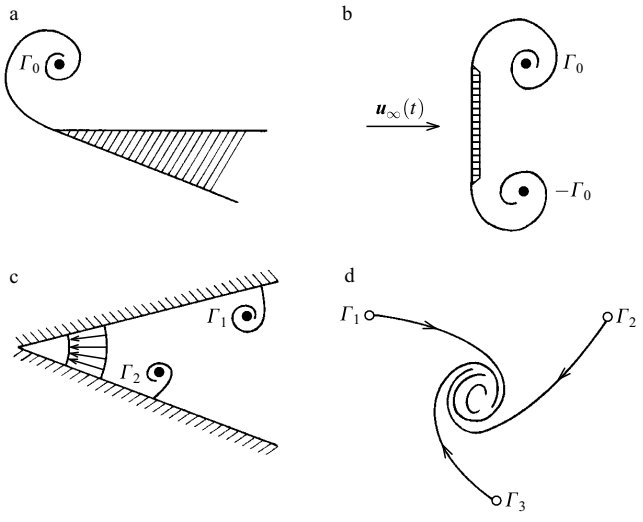

Figure 7. Examples of the Nikol'skii flow.

and rotate about the 'centre of gravity' $z = 0$. It follows from dimensional analysis that the angular velocity of rotation of the vortices is inversely proportional to the square root of time. Consequently, the solution can be represented in the form

$$z_j = b\sqrt{-t}\,\mu_1 \exp(\mathrm{i}\omega \ln t)\,, \qquad \Gamma_j = \frac{1}{2}\, b^2 G_j\,,$$

$$\mu_j = \xi_j + \mathrm{i}\eta_j\,, \qquad -\infty < t \leqslant 0\,.$$

The equations describing evolution can be converted to the algebraic form:

$$(2\mathrm{i}\omega + 1)\overline{\mu_j} = \sum_{k \neq j} \frac{G_j}{\mu_k - \mu_j}\,.$$

There are six real equations for eight real constants, which are obtained when ten unknowns ξ_j, η_j, Γ_j, and ω are reduced to the dimensionless form. There is, however, a solution to this underdetermined problem.

Further continuation of this solution in the direction of positive values of t can be regarded as unravelling (unrolling) of a vortex. In this case the directions of the arrows in Fig. 7d should be reversed. In contrast to collapse of vortices, which can be checked experimentally, such unravelling is not a natural causal process. Irreversibility is created in the dynamics of systems of point vortices when unravelling is impossible. This mechanism of the appearance of a 'time arrow' has no analogue in the dynamics of particles.

It seems almost self-evident that merging of vortices is unstable. Nevertheless, it would be of interest to determine the conditions of 'minimal instability' within the framework of a narrower definition of stability, such as that used by von Karman in an investigation of chains of point vortices [41, 42].

Is the collapse of two point vortices possible? The answer is yes [43]! This happens if point vortices simulate, as shown in Fig. 7b, separated flow, controlled by the Kutta conditions, from sharp or blunt edges of a body and the body collapses to form a point ($-\infty < t < 0$). The stability of such vortex merging seems to be almost self-evident.

Let us consider one more example of self-similar flow of an ideal fluid which is coevolution of a vortex sheet and a free boundary.

Although in the case of simultaneous evolution of different types of surfaces of tangential discontinuities of the velocity of an incompressible fluid the method of boundary integrodifferential equations allows superposition, studies of such problems meet with considerable numerical difficulties. An important practical example is the self-similar problem of oblique entry of a wedge into a water-filled lower half-space in accordance with a power-law time dependence. A free boundary *1* is adjacent to the sides of the wedge and a spiral vortex sheet *2* starting from the edge ensures that the Kutta condition of finite velocity is satisfied (Fig. 8a).

The method of matching asymptotic expansions leads, in the case of weak asymmetry, to separation of the phenomenon into two parts and each of them is characterised by just one type of discontinuity: in the outer region there is a free boundary and in the inner region, located near the wedge edge, there is a vortex sheet [44].

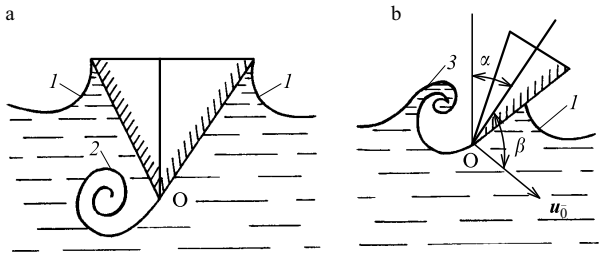

Figure 8. Entry of a wedge into water: (a) weak asymmetry; (b) strong asymmetry.

When the asymmetry parameters (which are the angle α between the vertical and the bisector of the wedge and the angle β between the bisector and the direction of the entry velocity $\boldsymbol{u}_0$) are sufficiently large, the flow pattern changes: a free boundary departs from the wedge edge O and it rolls up to a double spiral (*3*) because of a shock interaction with the wedge edge at the moment when the edge touches the water surface (Fig. 8b). Both flow patterns have to be checked experimentally as well as numerically.

3.3 Compressible fluid

The flow in the vicinity of the edge of a wedge or of the vertex of a cone can be self-similar also in the case of a compressible ideal medium. Three problems of this kind are known: diffraction of a shock wave by a wedge (Section 4.5), sudden acceleration of a wedge [45], and decay of an arbitrary wedge-shaped discontinuity [46]. Far from the wedge edge the flow is one-dimensional. As in the problem of oblique entry of a wedge into water, in asymmetric diffraction of a shock wave by a sufficiently thick wedge the Kutta condition can be satisfied within the framework of slip lines converging at the wedge edge and with their free lines rolled up to form a spiral.

For the same reason a spiral vortex slips off the wedge edge as a result of a sudden asymmetric motion from a state of rest in the regime in which a shock wave becomes detached.

The large number of dominant parameters has prevented so far the establishment of a topological classification of decay of an arbitrary wedge-shaped discontinuity even in the symmetric case. There are several ways of introducing asymmetry into the problem of decay of a wedge-shaped discontinuity. One can consider the evolution of an entity consisting initially of connected, to a common edge, N angular regions in each of which the parameters of gas differ. It is not clear whether in this case an N-turn spiral vortex is formed. We can assume that, for $t < 0$, supersonic flow with a centred rarefaction wave takes place around a 'solid wedge' and that inside the wedge the gas is at rest; at the instant $t = 0$ the wall wedges are removed.

The problem of an incompressible fluid is formulated similarly: at $t < 0$ the coordinate dependence of the complex velocity is represented by a power law. A vortex sheet, a free boundary, or a contact discontinuity can be selected as a slip line which coincides initially with the sides of a wedge [47].

Decay of an initially conical discontinuity is a difficult problem [48] and in the asymmetric (three-dimensional) variant it is hardly capable of exhaustive analysis.

3.4 Spiral vortex sheets

Before we consider self-similar spiral flow, we must consider helicity in general, digressing far from fluid dynamics, in full agreement with the principle that one who understands hydrodynamics alone does not understand it fully. The world surrounding us is spiral. There are numerous examples of spiral structures in animate and inanimate nature. The shells of garden snails, found in abundance at the roadside, are spiral. Spiral fossils have come to us from prehistoric times. Sunflower seeds form two families of oppositely twisted spirals. In technology there are spiral revolving knives, gears, etc. There is also the spiral shape of flowers and ferns, which cannot support themselves without rocks, building, or other plants. The horns of goats are twisted in opposite spirals.

Helicity is the fundamental property of matter, not only in the macroworld. In the microworld, we have the helical structure of the DNA molecule and in the megaworld we have spiral galaxies.

Spiral shapes are so frequent in nature that it is not possible to even list them all. Spiral waves are formed as a result of what is called spin detonation. They are also observed in the well-known Belousov–Zhabotinskii reaction. Many biologists believe that spiral waves account for arrhythmia in the operation of the heart muscle and in other biological phenomena. Spiral shock waves have been found in our and other galaxies. Three-dimensional spiral (more correctly, helical) structure is found in cyclones, water spouts, Ekman's flow above the surfaces of the oceans, and Taylor's flow in the upper atmosphere.

In the scientific sense, the helicity is used in two similar and dissimilar meanings. In physics, the helicity means the quantum number of an elementary particle, equal to the projection of its spin along the direction of its motion. In hydrodynamics this term, proposed by the English scientist Moffatt in 1969, denotes the scalar $\boldsymbol{u}\cdot\operatorname{curl}\boldsymbol{u}$ or a volume integral of this quantity, where $\boldsymbol{u}$ is the velocity vector of fluid particles. The helicity is conserved in an ideal fluid and its changes are due to kinks in the vortex lines and also due to diffusion. The helicity is used to describe cascade turbulence.

In each specific case a spiral structure usually represents some unsolved problem of natural science. However, in a more general synergetic sense, the spiral symmetry differs fundamentally from the symmetry of a snowflake, an atomic nucleus, or a chess position, and is a natural generalisation of the spherical symmetry. In contrast to the spherical symmetry, which is characterised by constant radius during rotation, the spiral symmetry is associated with contraction or elongation of the radius as it rotates clockwise or anticlockwise. Therefore, the spiral symmetry is a law of nature, whereas the spherical symmetry is an exceptional case.

Why the majority of the spiral shells and the helical DNA molecules are twisted in the same way? There is as yet no answer to this question. Since Pasteur, it has been agreed that such an unbalance of the spiral symmetry is a characteristic feature of life.

Philosophers have noticed long ago that art and science, balancing tradition against innovation, seem to develop along a spiral: the next turn of knowledge differs from the preceding one and yet they are alike. This analogy is symbolic but striking. Since it is qualitative and not rigorous, there are those who oppose it strongly:

''I don't think the scientists have got it right,
There is a hole, a gap, in their hypothesis.
The path of progress is not a spiral flight,
But aslant, oblique, spreading, and across it is.''
(V Vysotskii, translation by J Briggs)

This indeed may be so.

Let us now return to self-similar flow with spiral vortex sheets. The free end of a vortex sheet can roll up to form a spiral with an infinite number of turns. The asymptotic behaviour of the solution at the centre of a plane spiral vortex ($\theta \to \infty$, $r \to 0$) may be investigated by replacing the polar coordinates r, θ with r, η [where η is the spiral variable

$$0 \leqslant \eta = \theta - \theta_0(r) \leqslant 2\pi ,$$

$\theta_0(r)$ is the shape of a vortex sheet, and r is the self-similar coordinate] and expanding the functions as series in powers of r. This can be done if the function $\theta_0(r)$ is monotonic. An increase in η from zero to 2π for $r = \text{const}$ implies a circular path from one side of a vortex sheet to the other. Therefore, the spiral periodic condition is satisfied: the pressure and the velocity component normal to a vortex sheet are identical for $\eta = 0$ and $\eta = 2\pi$.

A spiral vortex sheet is logarithmic if the self-similarity index is $n < \frac{1}{2}$ [49] and algebraic if $n > \frac{1}{2}$ [50]. Numerical solutions of specific problems of separation of a vortex sheet from a solid surface [25] have been obtained only for algebraic spirals. The solutions obtained are due to the utilisation of a fortunate, characteristic of the nature of the problem itself, approximation of the core of a vortex sheet by a point vortex with a cut. Application of the same approximation to the core of a logarithmic spiral fails: the results of numerical calculations become unstable. This unsolved problem demonstrates also that fitting the results of numerical calculation to the well-known asymptote for a fold is one of the difficult problems in computational hydrodynamics.

It has been found experimentally that at the cores of spiral vortices, which become separated from the edges of a low-aspect-ratio wing in a water tunnel, cavitation zones form that are visible to the naked eye. According to the unsteady analogy, this conical flow is equivalent to plane flow ($n = 1$).

Cavities do not appear in a fluid which cannot exist in the drop form (for example, air or any other gas) and, in accordance with the asymptote of the flow at the centre of the core of a vortex sheet ($r \to 0$), the pressure p tends to $-\infty$ obeying the following logarithmic law:

$$p \simeq p_0 + \rho u_0^2 \ln r ,$$

where p_0 and u_0 are the certain characteristic values of the pressure and velocity.

The order of the size of a cavity in a fluid that forms drops (for example, water) is small† if the cavitation number

$$\sigma = 2\,\frac{p_0 - p_1}{\rho u_0^2}$$

is large (p_1 is the pressure in the cavity). The large parameter σ characteristic of this unsolved problem means that an asymptotic approach has to be followed.

†The region where diffusion is important is of characteristic size $\sim(\nu t)^{1/2}$. Therefore, it can be assumed that, for large values of Re, the viscous flow region is located near the top of the wing ($t \ll 1$).

The problem requires generalisation to the case of flow with the self-similarity index $n \neq 1$, selected from the range $0.5 < n < 1$, when the pressure in the region external to a cavity tends to $-\infty$, obeying a power law, as r is reduced [50].

If the size of a cavity is comparable with the size of a body immersed in fluid flowing past it, the helicity is not an appropriate concept. The exact solution of the problem had been obtained by von Karman for the case of pseudosteady ($n = 0$) symmetric flow past a plate [51]. It is not clear when the point of closure of a cavity is located on the symmetry line and when it is on the body.

Can the Prandtl solution for a logarithmic vortex sheet [49] be generalised to the case of flow of a compressible gas? The answer has not yet been found.

The Euler equations

$$u_t + uu_R + \frac{1}{R}\,vu_\theta - \frac{1}{R}\,v^2 = -\frac{1}{\rho}\,p_R ,$$

$$v_t + uv_R + \frac{1}{R}\,vv_\theta + \frac{1}{R}\,uv = -\frac{1}{R\rho}\,p_\theta ,$$

$$\rho_t + \frac{1}{R}\,(R\rho u)_R + \frac{1}{R}\,(\rho v)_\theta = 0 ,$$

$$S_t + uS_R + \frac{v}{R}\,S_\theta = 0 ,$$

where u and v are the components of the velocity along the directions of R and θ, $S = p\rho^{-\gamma}$ is the entropy function, and γ is the adiabatic exponent, have (or do not have!) the exact solution

$$u(R, \theta, t) = n\,\frac{R}{t}\,\big[U_0(\eta) + 1\big] ,$$

$$v(R, \theta, t) = n\,\frac{R}{t}\,V_0(\eta) ,$$

$$\rho(R, \theta, t) = \rho_0(\pm t)^{q\varepsilon} r^{\varepsilon - 2}\rho_0(\eta) ,$$

$$p(R, \theta, t) = n^2\rho_0 b^2(\pm t)^{qn - 2 + 2n} r^{\varepsilon} p_0(\eta) ,$$

$$R = b(\pm t)^n r , \qquad 0 \leqslant \eta \leqslant \eta_0 , \qquad \theta_0 = -k \ln r .$$

Instead of U_0 and V_0, we shall introduce now the components of the relative velocities U and V which are equal to the normal and tangential components on a slip line:

$$(1 + k^2)^{1/2}\,U = V_0 + kU_0 , \qquad (1 + k^2)^{1/2}\,V = kV_0 - U_0 .$$

The unknown functions U, V, p_0, and ρ_0 can be found from the Euler equations by deriving a system of ordinary differential equations:

$$(a^2 - U^2)U' = A , \qquad UV' = B ,$$
$$(a^2 - U^2)p_0' = Cp_0 , \qquad U(a^2 - U^2)\rho_0' = D\rho_0 ,$$

where $a^2 = \gamma T$, and the functions A, B, C, and D are algebraic polynomials which depend on U, V, and $T = p_0/\rho_0$.

The following periodicity conditions are satisfied on a vortex sheet ($\eta_0 = 2\pi$):

$$p_0(0) = p_0(2\pi) , \qquad U(0) = U(2\pi) = 0 .$$

There is also a problem of rolling up, into a logarithmic spiral, of two free boundaries:

$$\theta_1(r) = -k \ln r, \quad \theta_2(r) = \eta_0 - k \ln r .$$

The following conditions of constant pressure and zero velocity are satisfied on these boundaries:

$$p_0(0) = p_0(\eta_0) = p^0, \quad U(0) = U(\eta_0) = 0, \quad \eta_0 < 2\pi .$$

The system of ordinary differential equations under investigation has two singularities. Continuous passage across the singularity $\eta = \eta_1$ $(0 < \eta_1 < \eta_0)$, where $a = \pm U$, is possible only if $A = 0$. The other singularity, $U = 0$, is located on a slip line. For finite values of $T(0)$ the derivative $U'(0)$ is finite.

It is not known whether there exists a similar solution for a vortex sheet in the shape of an algebraic spiral in a compressible gas [52].

3.5 Viscous fluid

The interaction of a shock wave with a boundary layer that is formed as a result of a strong point explosion on a plane is a problem with important applications and it has been completely ignored. Fig. 9 shows the shapes of an explosive charge and of a shock wave for the plane $(N = 1)$, cylindrical $(N = 2)$, and spherical $(N = 3)$ symmetries. The cylindrical symmetry is possible when the line formed by an explosive charge is perpendicular to a plane P (fig. 9b) and when this line lies in the plane P (Fig. 9c). The flow is self-similar if, in accordance with expression (3.1), we have $k = -\frac{1}{2}$ for $N = 1$, $k = 0$ for $N = 2$, and $k = \frac{1}{6}$ for $N = 3$. The determining parameter is the Reynolds number

$$Re = \left(\frac{E}{\rho}\right)^{1/N} \frac{\mathcal{R}^k}{\nu_1},$$

where E is the energy released by such an explosion, ρ is the density of the undisturbed gas, and $\mathcal{R}$ is the gas constant.

In the limit $Re \to \infty$, a boundary layer forms in the plane P. Singular regions where the concept of a boundary layer breaks down are located near the epicentre of the explosion and in the region of interaction of the shock wave with the boundary layer. Does this interaction crate a shock-wave precursor?

One further example of self-similar flow of a viscous liquid is the Stewartson problem of the motion of a semi-infinite plate parallel to itself from rest at a velocity nbt^{n-1} [53]. If the velocity is not directed along the normal to the plate edge, we are faced with the problem of unsteady flow past a sliding plate.

If the boundary layer concept is adopted $(Re \to \infty)$, any value of the self-similarity index is permissible in the Stewartson problem, whereas on the basis of the Navier–Stokes equation only those values of the index are allowed which satisfy the condition described by expression (3.1). The principle of maximum simplicity can be applied a priori before numerical calculations are carried out. The simplest field of self-similar paths obtained in this way has five singularities (two saddles S and three node N). It is plotted in Fig. 10 on the assumption that a low-viscosity liquid $(Re \to \infty)$ *runs into the edge* $(b > 0)$ [54]. Perturbations do not penetrate the limiting line $x = bt^n$ and the influence of the top of the plate is negligible in the region $x > bt^n$: the one-dimensional solution obtained a long time ago by Rayleigh [6] applies here. It is not clear what is the topology of self-similar paths in the problem of the flow *running off* $(b < 0)$ from the edge of a flat plate and how does it vary with Re.

Limiting lines appear also in a stationary three-dimensional boundary layer [55]. The solution near a limiting line has not yet been obtained.

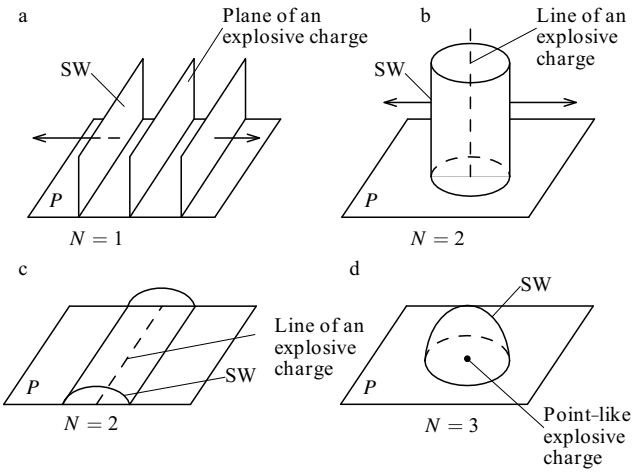

Figure 9. Problem of a strong explosion of a charge located on a plane $(N = 1)$, on a line $(N = 2)$, and at a point $(N = 3)$; SW is shock wave.

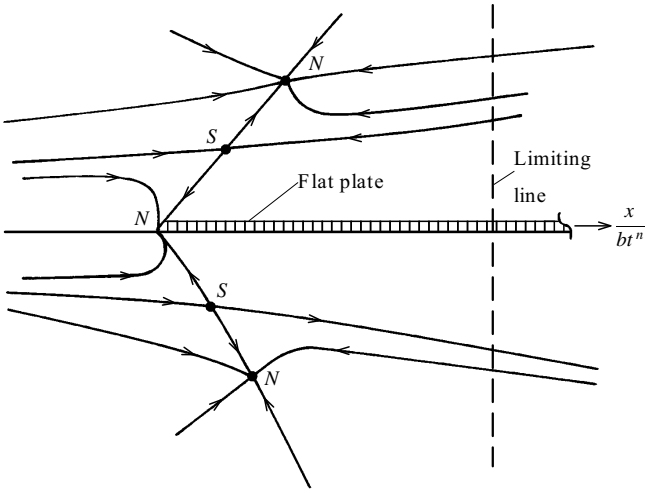

Figure 10. Field of self-similar paths in the Stewartson problem.

3.6 Two comments about self-similar solutions

We have considered so far only the self-similar solutions satisfying exactly the Euler, Navier–Stokes, or Prandtl equations. However, there is a whole class of approximately self-similar solutions which exist in a certain local space–time region. They are the asymptotically self-similar solutions.

Let us assume that a solution

$$\boldsymbol{u}(\boldsymbol{r}, t) \simeq \frac{1}{a} \boldsymbol{U}(\boldsymbol{R}) , \qquad (3.2)$$

where $\boldsymbol{r} = b\boldsymbol{R}$, $a(t) > 0$, $b(t) > 0$, is valid for $t \to t_0$, $R = O(1)$. Then if $a = b$ and $|a'|a \ll 1$, this solution satisfies the Navier–Stokes equation (if $|a'|a = 1$, we obtain the exact Birkhoff solution). If $a \ll b$, it satisfies the Euler equation (for $|a'|b = |b'|a$ we have the exact solution), and if $a \gg b$, it satisfies the Stokes equation.

The Stokes equation describes, for example, an exponential approach of the solution to the state of rest:

$$a = \exp(kt), \quad b = 1, \quad k > 0, \quad t \to \infty .$$

Substitution of the solution represented by expression (3.2) into Eqn (2.5) and neglect of the quadratic terms gives

$$\nu\nabla_R^2 \boldsymbol{U} + k\boldsymbol{U} - \nabla_R P = 0, \quad \nabla_R \cdot \boldsymbol{U} = 0 , \tag{3.3}$$

where

$$p(\boldsymbol{r}, t) = \exp(-kt) P(\boldsymbol{R}) + o\left[\exp(-kt)\right] .$$

Such a linear system of equations describes the flow of a fluid in bounded and unbounded regions, for example, rotation of tea in a glass after stirring, the flow near a body when it comes to rest, slowing down of rotation of a wingless rocket, etc. The boundaries of solids may be at rest or they may be moving at an exponentially decreasing velocity. In the case of symmetric rotation of a liquid relative to the $r = 0$ axis, the system of equations (3.3) reduces to the Bessel equation:

$$ru_0''(r) + u_0'(r) + \frac{k}{\nu} ru_0(r) = 0 .$$

The second comment applies to unbounded solutions. The space–time singularity of the solution, called by physicists the unbounded cumulation and the peaking regime by mathematicians, can be divided into the three types listed below.

(1) *The solution is unbounded in the whole space at $t = 0$.* For example, Eqn (2.5) has (or does not have?) the solution

$$\boldsymbol{u}(\boldsymbol{r}, t) = \frac{1}{t}\,\boldsymbol{u}_0(\boldsymbol{r}) + o\left(\frac{1}{t}\right), \quad p(\boldsymbol{r}, t) = \frac{1}{t^2}\,p_0(\boldsymbol{r}) + o\left(\frac{1}{t^2}\right) .$$

There is no dissipative term in this approxinmation:

$$-\boldsymbol{u}_0 + (\boldsymbol{u}_0 \cdot \nabla)\boldsymbol{u}_0 = -\frac{1}{\rho}\nabla p, \quad \nabla \cdot \boldsymbol{u}_0 = 0 .$$

The following simple example demonstrates that the nonlinear heat conduction equation allows the appearance of a singularity in a finite time:

$$u_t = uu_{xx} , \quad u = \frac{a_0 + a_1 x - x^2}{2t} .$$

(2) *The solution is unbounded at any time on a singular low-dimensional manifold, representing a surface, a line, or a point.* Examples of such singularities are a vortex filament, a line of sources, the solution of the Navier–Stokes equation for $|\boldsymbol{u}| = O(r^{-1})$ when $r \to 0$, and the convective term $(\boldsymbol{u} \cdot \nabla)\boldsymbol{u}$ the modulus of which is of the same order of magnitude as the term $\nu|\nabla^2 \boldsymbol{u}| = O(r^{-3})$.

Near the centre ($r = 0$) of a self-similar point explosion in an ideal gas the velocity u and the density ρ tend to zero [31]:

$$u = c_1 \frac{r}{t} + o(r) ,$$

$$\rho = c_2 t^{-2N/[(N+2)(\gamma-1)]}\, r^{N/(\gamma-1)} + o\left(r^{N/(\gamma-1)}\right) ,$$

where r is the radial coordinate, and c_1 and c_2 are constants. The pressure at the centre of the explosion is finite, but the temperature tends to infinity. Therefore, the model of a perfect gas becomes invalid and near the epicentre of the explosion we have to take into account the effects of heat conduction and viscosity. The simplest model makes it possible to apply the hypothesis of self-similarity. If $Re \gg 1$, the influence of heat conduction and viscosity is concentrated near the epicentre, i.e. in the inner region. In the outer region the solution of the problem of a point explosion in an ideal medium applies.

(3) *Unbounded solution for $r = t = 0$.* One example is the Guderley problem of the focusing of a cylindrical or spherical shock wave at the point $r = 0$ at the instant $t = 0$ [32].

The Rayleigh problem of the collapse of bubbles in an incompressible fluid is interesting because at the moment of focusing ($t = 0$) the velocity is infinite only at the point $r = 0$, whereas the pressure is infinite throughout the region of flow. Therefore, this problem can be regarded as of the first or third type. In some cases, for example, in the problem of a shock wave reaching the upper boundary atmosphere [32], the pressure is finite, but the temperature is infinite.

These infinity paradoxes are a consequence of using mathematical models which are far too simplistic, but these paradoxes can be resolved if we take account of real properties of a fluid such as dissipation, second viscosity, compressibility, thermodynamic imperfections of a medium, relaxation, emission of radiation, etc. There is always some, no matter how small, factor which when included makes the solution bounded: nature does not tolerate infinities. For example, the collapse of a cylindrical bubble in an incompressible fluid stops with slow rotation [56].

4. 'Dry water' model

In Fig. 4 the 'wet water' model is represented by the two columns on the left and the 'dry water' model by the three columns on the right.

The 'dry water' model has been studied actively throughout the whole history of hydrodynamics. However, the flow of a zero-viscosity fluid differs significantly from that of a real fluid. The two types of flow are identical only in cases which are an exception to this rule: the 'dry water' model does not explain the main problem which is the appearance of vortices in an incompressible fluid in the presence of external potential forces. The reason for this is that, as the viscosity approaches zero, its effect does not vanish completely and remains in small subregions (boundary and mixing layers), thus influencing significantly the flow as a whole.

4.1 Three-dimensional vortices

Vortices in a viscous fluid merge because of diffusion. There is no diffusion in an ideal fluid. Therefore, merging of vortices in such a fluid is one of the surprising properties of vortex clusters. A numerical calculation has been made [57] of the evolution of two vortices with the same sign in an incompressible liquid. Each of these vortices is initially in the shape of a circle of radius r and has a constant angular velocity ω_0. When the dimensionless initial distance l/r between vortices is sufficiently large,

they expand into ovals and rotate separately, like point vortices (this analogy is valid for $l \gg r$), around a geometric centre. When the initial distance between the vortices is small, they merge to form a single tangle in a finite time. In the critical case corresponding to $l/r \approx 3.2$ the vortices are in periodic motion: partly merging and then diverging.

Details of how vortices merge are not clear. It is assumed that it is a contact process: in a finite time the minimum distance between vortex regions vanishes, as shown in Fig. 11a, where the vortices are shown shaded.

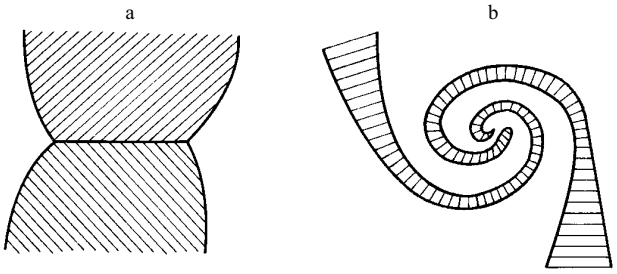

Figure 11. Patterns of merging of two three-dimensional vortices.

Two-spiral capture is also a priori self-consistent: regions occupied by vortices alternate with those which are free of vortices and the connectivity of space is conserved (Fig. 11b).

When the number of point vortices exceeds three, a transition to chaos takes place [58]. This means that chaos is definitely possible in a system of distributed vortices if the connectivity of a vortex-free potential region exceeds four. Examples of steadily rotating vortices are the Kirchhoff elliptical vortex, as well as its various one-parameter generalisations in the form of single and double vortex structures known as Burbea's patches [59, 60]. The search for other vortices is continuing.

It seems likely that the connectivity of a vortical region can increase or decrease in the course of its evolution.

The critical value of l/r for a compressible perfect gas depends on the adiabatic exponent and on the 'Mach number' $\omega_0 r/a_0$, where a_0 is the velocity of sound at infinity. Problems of this kind can not only provide tests of numerical methods dealing with inviscid flow, but they may be also a source of new knowledge about the appearance of acoustic lines and shock waves during evolution of vortices.

Another simple example is that of a thin vortical jet. It would seem that the solution is not difficult to obtain: the flow in such a jet should be described by the thin-layer equation:

$$uu_x + vu_y = -\frac{1}{\rho}\, p'(x)\ ,$$

where the pressure $p(x)$ is constant over a transverse section across the layer [$u(x, y)$, $v(x, y)$ are the velocity components along the jet axis x and along the normal y to the jet]. Although this equation has a quadrature in the form of an analogue of the Bernoulli integral

$$\frac{p}{\rho} + \frac{1}{2}\, u^2 = f(\psi)\ ,$$

where $-f'(\psi) = -\psi_{yy}$ is the vorticity and θ is the stream function ($u = \psi_y$, $v = -\psi_x$), this asymptotic approach is invalid in singular flow regions where the initial assumptions of a small thickness of the flow region are not obeyed. This is true in the vicinity of the stagnation points A on a body, sharp edges B of a body, and points of separation and reattachment C (Fig. 12). The boundary of a jet may also be the subject to surface tension forces.

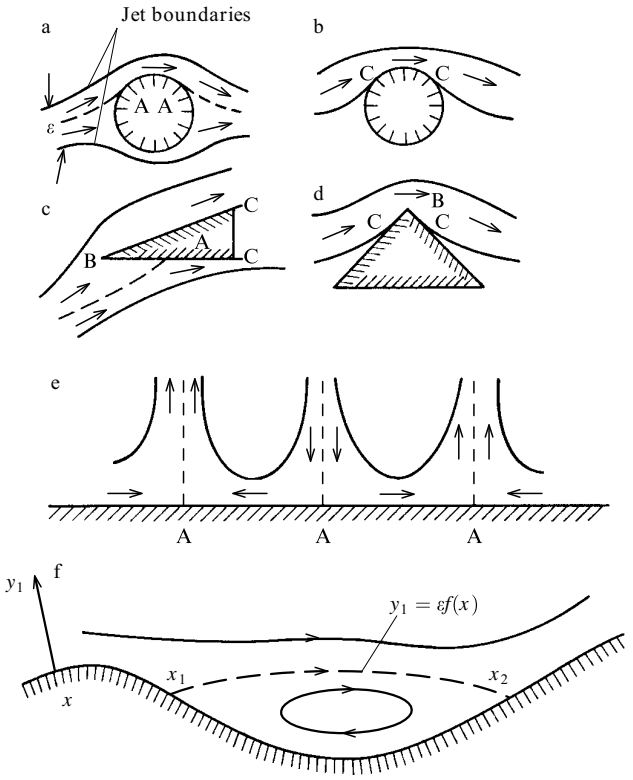

Figure 12. Jet flow patterns.

It follows that the thin-layer theory of an ideal fluid is far from complete both in planar and three-dimensional cases [61]. It would be of interest to consider the separation of a thin jet from a body. Two different formulations of the problem are possible. If this jet is immersed in a liquid at rest (immersed jet), its boundary is free. If the jet is surrounded by a moving liquid, its boundary is a contact discontinuity.

Formation of a bubble, which is a closed circulation zone, in the flow of an inviscid liquid is problematic. Nevertheless, it is possible to estimate quite simply the shape of a thin bubble in the flow of an inviscid liquid which is not subject to surface tension forces (Fig. 12f). The thin-layer approximation is valid:

$$\psi(x, y_1; \varepsilon) = \varepsilon \Psi(x, y) + o(\varepsilon)\,, \qquad y_1 = \varepsilon y\ ,$$

where $\varepsilon \ll 1$ is the flatness coefficient of the bubble.

It follows from the Batchelor theorem [6] that the vorticity is constant inside the bubble:

$$\Psi = y u_0(x) - \frac{1}{2}\, y^2 \Omega\,, \qquad \Omega = \varepsilon\, \omega\ ,$$

$$p(x) = p_0 - \frac{1}{2}\, \rho u_0^2(x)\,, \qquad p_0 = \text{const}\ .$$

We shall assume that the bubble boundary is described by the equation $y_1 = \varepsilon f(x)$. Outside the bubble the flow is vortex-free:

$$\Psi = \left[y - f(x)\right] u_1(x), \qquad p(x) + \frac{1}{2}\rho u_1^2(x) = \text{const}\ .$$

The pressure distribution $p(x)$ is assumed to be given and it is created by external factors. It follows from the condition $\Psi(x, f) = 0$ that the bubble shape is

$$f(x) = -\frac{2}{\Omega}\sqrt{2\frac{p_0 - p}{\rho}}\ .$$

Since $f(x_1) = f(x_2) = 0$, the pressure $p(x)$ has a maximum in the region where the bubble is located (x_1, x_2).

4.2 Vortex sheets

If a problem can be reduced to a boundary equation, its dimension decreases by unity and the equations become two-dimensional. Therefore, modern computers can be used to solve more complex problems than those that are soluble directly by the difference methods, finite element methods, etc. The method of boundary integral equations, which is a modern version of the potential method, has become popular in the solution of steady-state problems in the mechanics of continuous media. It is not always possible to reduce equations describing unsteady motion to integral equations, because the former contain a time derivative. Therefore, there is a chance to obtain boundary integrodifferential equations. This is used in the case of flow of incompressible fluids.

The contributions to the velocity $\boldsymbol{u}$ made by vortices distributed in space and by those concentrated on a tangential discontinuity surface add up together. We shall consider only the latter. Let us assume that a single vortex sheet, described by the equation $\boldsymbol{r} = \boldsymbol{R}(\xi, \Gamma, t)$, evolves in a vortex-free potential; here Γ is the circulation measured from a certain centre and ξ is a coordinate along the $\Gamma = \text{const}$ vortex line. The physical meaning of a vortex sheet is that it is vortex $\boldsymbol{\omega}$ of infinite strength and concentrated on a $\boldsymbol{r} = \boldsymbol{R}^0$ surface. It follows from the Biot–Savart formula

$$\boldsymbol{u}(\boldsymbol{r}, t) = \frac{1}{4\pi}\int \frac{(\boldsymbol{r}^0 - \boldsymbol{r}) \times \boldsymbol{\omega}^0}{|\boldsymbol{r}^0 - \boldsymbol{r}|^3}\,\mathrm{d}\tau^0\ ,$$

where $\mathrm{d}\tau = \mathrm{d}\eta\,\mathrm{d}S$ is an element of volume and $\mathrm{d}S$ is an element of the area of a surface vortex, that if

$$\lim_{\omega\to\infty,\,\Delta\eta\to 0}(\omega\Delta\eta) = \boldsymbol{\gamma}\ ,$$

then

$$\boldsymbol{u}(\boldsymbol{r}, t) = \frac{1}{4\pi}\int \frac{(\boldsymbol{R}^0 - \boldsymbol{r}) \times \boldsymbol{\gamma}^0}{|\boldsymbol{R}^0 - \boldsymbol{r}|^3}\,\mathrm{d}S^0\ , \tag{4.1}$$

where $\boldsymbol{u}^+ - \boldsymbol{u}^- = \boldsymbol{\gamma} \times \boldsymbol{n}$ is a discontinuity of the velocity vector on a vortex sheet and $\boldsymbol{n}$ is a unit normal to this sheet.

What is the velocity of a vortex line characterised by $\Gamma = \text{const}$? It follows from the condition of continuity of the pressure on a vortex sheet and from the Bernoulli equation that

$$\frac{\partial\Delta\varphi}{\partial t} + \frac{\boldsymbol{u}^+ + \boldsymbol{u}^-}{2}\nabla(\Delta\varphi) = 0\ ,$$

where $\Delta\varphi = \varphi^+ - \varphi^- = \Gamma$ is the difference between the potentials on a vortex sheet. It therefore follows that a vortex line is travelling at a velocity $(\boldsymbol{u}^+ + \boldsymbol{u}^-)/2$.

According to the Sokhotskii formula, the principal value of the singular integral described by Eqn (4.1), found for the case when the point at which the velocity is calculated is located on the vortex sheet itself, is equal to the half-sum of the velocities on opposite sides of the sheet. Therefore, the equation of evolution is

$$\frac{\partial\boldsymbol{R}(\xi, \Gamma, t)}{\partial t} = \frac{1}{4\pi}\int \frac{(\boldsymbol{R}^0 - \boldsymbol{R}) \times \boldsymbol{\gamma}^0}{|\boldsymbol{R}^0 - \boldsymbol{R}|^3}\,\mathrm{d}S^0\ . \tag{4.2}$$

The shape of a plane vortex sheet can be represented in the form $z = z(\Gamma, t)$, where $z = x + \mathrm{i}y$ is a complex coordinate. It follows from Eqn (4.2) that

$$\frac{\partial\overline{z(\Gamma, t)}}{\partial t} = \frac{1}{2\pi\mathrm{i}}\int \frac{\mathrm{d}\Gamma^0}{z(\Gamma^0, t) - z(\Gamma, t)}\ .$$

The term 'singular integral' is understood to be here the Cauchy principal value and the bar in the above expression represents complex conjugation. The presence of a body in a flowing fluid is particularly easy to take into account when the region of flow is transformed into a half-plane or a circle by conformal mapping $\zeta = \zeta(z, t)$. Conjugate vortex sheets are included in this more general case and the equation of evolution becomes

$$a\frac{\partial\overline{\zeta_k(\Gamma, t)}}{\partial t} = b(\zeta_k, t) + \frac{1}{2\pi\mathrm{i}}\sum_n \int \frac{\mathrm{d}\Gamma^0}{\zeta_n(\Gamma^0, t) - \zeta_k(\Gamma, t)}\ , \tag{4.3}$$

where $a = |\partial z/\partial\zeta|^2$ is the square of the modulus of the stretching of the coordinates and b is the complex velocity of flow in the absence of vortex sheets.

Eqns (4.2) and (4.3) have not yet been studied by mathematicians.

We can go over to flow characterised by point vortices if the solution can be represented in the form of the δ function:

$$\frac{\mathrm{d}\Gamma^0}{\mathrm{d}\zeta_n} = \Gamma_n\delta(\zeta - \zeta_n)\ .$$

In this case the Cauchy integral can be replaced with an algebraic expression and the integrodifferential equation (4.3) reduces to differential.

The equation of evolution of tangential discontinuities leads in a natural manner to an autonomous problem with initial data, i.e. it is not related directly to the viscosity effects, and it is formulated as follows: it is necessary to find the geometry and intensity of a discontinuity for $t > 0$ provided they are known for $t = 0$. The problem whether this formulation is ill-posed is fundamental. A vortex sheet is always unstable, whereas a contact discontinuity and a free boundary are unstable in the absence of stabilising factors. A mathematical manifestation of this instability is an ill-posed problem. In fact, small short-wavelength perturbations such as a travelling wave

$$y_0 = \exp\left(\omega t - \mathrm{i}\omega\frac{x}{u_0}\right)$$

[where $y = y_0(x, t)$ is the shape of the discontinuity and $\pm u_0$ is the velocity of the fluid on its opposite sides] satisfy the Laplace equation

$$\frac{\partial^2 y_0}{\partial t^2} + u_0\frac{\partial^2 y}{\partial x^2} = 0\ ,$$

when the problem with the initial conditions is ill-posed in the Hadamard sense [62].

It is known that ill-posedness is a constant feature of *inverse problems*. A steady-state inverse problem in hydrodynamics is determination of the shape of a body past which a fluid is flowing, either from the distribution of the pressure on this body [63] or from the shape of a shock formed ahead of the body [64, 65]. The problem of determination of the shape of the surface of a tangential discontinuity (with a given shape of a body) is direct.

The necessary condition for a well-posedness (which is that the solution should depend in a continuous manner on the initial data and on external factors) of evolution problems is the requirement of analyticity of an interface. A solution which is conditionally correct, i.e. piecewise analytic, can be obtained by special regularisation methods [22, 66]. A regulariser cuts off the hf harmonics of a Fourier series, smooths out short-wavelength perturbations, and does not reduce a given precision of a numerical calculation procedure. Let us consider the effect of one of the regularisers on the Hadamard example:

$$u_{tt} + u_{xx} = 0\,, \qquad u(x,\,0) = 0\,, \qquad u_t(x,\,0) = \delta \sin(nx)\ .$$

The solution

$$u(x,\,t) = \frac{\delta}{n} \sinh(nt) \sin(nx)\ ,$$

defined in the finite time interval $0 < t < 1$, increases exponentially in the limit $n \to \infty$. Let us add to the equation a regulariser in the form a fourth-order derivative of the required function:

$$u_{tt} + u_{xx} + \varepsilon^2 u_{xx\,xx} = 0\ .$$

The task is to determine a value of $\varepsilon(\delta)$ which would satisfy the conditions

$$\lim_{\delta \to 0} \varepsilon = 0\,, \qquad \lim_{n \to \infty,\, \delta \to 0} u(x,\,t) = 0\ .$$

For the solution given by

$$u(x,\,t) = \frac{\delta}{k} \sinh(kt) \sin(nx)\,, \qquad k = n\sqrt{1 - \varepsilon^2 n^2}$$

the estimate looks as follows:

$$\left|u(x,\,t)\right| \leqslant \frac{\delta}{k_{\max}} \sinh k_{\max} = 2\varepsilon\delta \sinh \frac{1}{2\varepsilon}\ , \qquad k_{\max} = \frac{1}{2\varepsilon}$$

(in the Hadamard example, we have $k_{\max} = \infty$). Therefore

$$\lim_{\delta \to 0} u(x,\,t) = 0\,, \qquad \text{if} \quad \lim_{\delta \to 0} \left(\varepsilon\delta \exp \frac{1}{2\varepsilon} \right) = 0\ .$$

Here, we can select $\varepsilon(\delta)$ e.g. in the form of the function

$$\varepsilon = -\frac{1}{2 \ln \delta}\ .$$

This example of regularisation, based on introduction of an even high-order derivative, is just the simplest illustration of the mechanism of action of a linear regulariser [62] based on additive introduction, into the equation of evolution of a vortex sheet [Eqn (4.3)], of the term

$$\varepsilon^2 \frac{\partial^2 \overline{z(\Gamma,\,t)}}{\partial \Gamma^2}\ .$$

There is an uncountable number of regularisation methods. Apart from the linear regularisation method, the method of an artificial vortex layer [67] and the method of rediscretisation [68] have proved themselves in practice. It is suggested in Ref. [69] that the surface tension be used as a regulariser. It seems that such a regulariser would not be very effective: when the surface tension is low, no stabilisation takes place. The choice of the optimal regulariser is a topical problem in computational hydrodynamics.

The method of boundary integrodifferential equations has to be generalised to the cases of axisymmetric flow of an incompressible fluid [70] and of plane flow of a compressible fluid [71].

4.3 Free boundaries

The equation for a plane contact discontinuity can be represented in the form $z = z(\sigma,\,t)$, where the constant value of the parameter σ is conserved across this discontinuity and identifies a point moving at a velocity $(\boldsymbol{u}^+ + \boldsymbol{u}^-)/2$. The point $\Gamma = \text{const}$ does not move at the same velocity. Therefore, a system of two equations is needed for the determination of two functions $z(\sigma,\,t)$ and $\Gamma(\sigma,\,t)$ defined at the discontinuity. These equations have been derived with account taken of the surface tension, the forces due to gravity, and the difference between the densities $\rho^{\pm}$ and between the Bernoulli constants of the fluids in contact both in the case of periodic waves [69] and for a closed contact discontinuity [22]. Preliminary attempts have been made to obtain a numerical solution of the system of equations of evolution of a contact discontinuity.

This system of equations is valid if $\rho^+\rho^- \neq 0$ and, in principle, it does not differ from the system of equations of evolution of a free boundary. The latter cannot be obtained by going to the limit $\rho^+ \to 0$ or $\rho^- \to 0$ because the area bounded by a contact discontinuity — in contrast to the area bounded by a free boundary, i.e. the area of a cavity — is invariant in a solenoidal field of flow. An integrodifferential equation of evolution of a free boundary, regarded as a line of vortex sources on a plane, was introduced in Ref. [22] and integral equations are discussed in Ref. [72].

There are many unsolved problems relating to the formation of steady separated flow. For example, we can imagine the following scenarios of steady flow with two free boundaries starting from a body in flow: expansion of a closed cavity, expansion of two closed cavities followed by their merging into one, growth of two accelerating Prandtl vortices and their merging at infinity. At the final stage ($t \gg 1$) of evolu-tion of cavitational flow a cavity shrinks into a section of a straight line and the body in a flowing fluid shrinks to a point where the singularity is determined by the drag coefficient.

Let us now consider some specific problems.

In 1910 an aircraft of unusual design was test-flown successfully not far from Paris. It did not have an obligatory (at the time) propeller and instead its nose contained a compression engine, which was the prototype of a modern air-breathing jet engine! The young Rumanian designer of this aircraft, by the name of Coanda, placed metallic shields to protect the plywood fuselage from the flames shooting out from the jet nozzles. How surprised he must have been when the jet became sucked towards the fuselage instead of being deflected from it.

The phenomenon of a slow jet deviating greatly from its direction which at a high flow rate is known as the Coanda effect and also as the teapot effect. We encounter this effect every day: at low angles of tilt of the teapot the tea emerging from it follows the shape of the spout and its flow assumes various forms.

The Coanda effect can be observed in planar flow in an open trough. It is hardly possible to realise planar flow in its pure form (is this not typical of hydrodynamic phenomena?), but a priori we can assume that, apart from the case of a layer which becomes attached to the outer surface of a plate (Fig. 13a) and the case of a free jet (Fig. 13b), there is an intermediate regime in a wide range of flow rates in which a planar jet splits, like an axisymmetric one, into wall and free parts (Fig. 13c). The solution of the Euler equation for the first two cases does exist, but nor for the case shown in Fig. 13c.

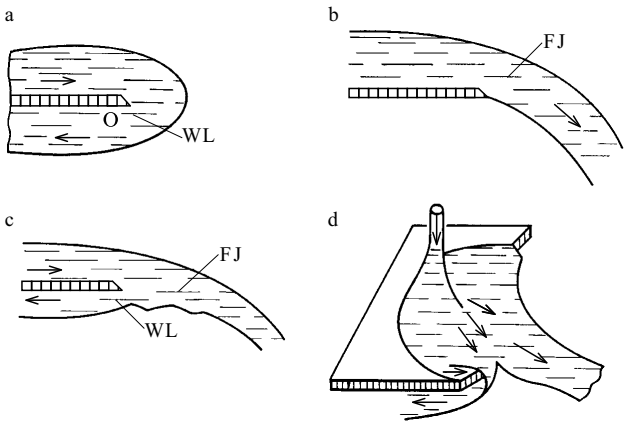

Figure 13. The Coanda effect. WL is a wall layer and FJ is a free jet.

All types of flow past a body can be observed simultaneously (shown in Fig. 13d) if a rectangular plate is inserted into a stream of water coming from a tap.

It is traditionally assumed that the problem of a plane stream flowing past a sharp edge can be formulated on the basis of the 'dry water' theory [73, 74]: the difference between the atmospheric pressure at the free boundary of the stream and the theoretical infinite rarefaction at the edge of the plate (O in Fig. 13a) presses the stream against the plate. However, if $Re = q/\nu \gg 1$ (q is the rate of flow in the jet), a boundary layer can separate under the action of an unfavourable (decelerating) pressure gradient on the lower surface of a plate. Therefore, the influence of viscosity is important.

Near the edge of a plate there is always a region where the complete Navier–Stokes equation cannot be simplified. The situation resembles the familiar unsolved problem of the flow of a fluid near the front and rear edges of the plate at which a Prandtl–Blasius boundary layer is formed [75]. In the latter case there is a coordinate expansion which is valid in the vicinity of the edge [75, 76] and which does not overlap the solution in a region where the Navier–Stokes equation is valid and even less so where the Prandtl equation applies. A natural generalisation of this problem is the flow past a corner edge.

A free film of a fluid which is accelerating, for example under the action of the force of gravity, becomes thinner and eventually breaks up. One of the ways in which this can happen is the rolling up of a film into a system of streams. The solution in the vicinity of the edge of a free film, like that near the 'point' of formation of the streams, is not known. The number of streams is not known either. It is claimed in Ref. [14] that the system can consist of one, two, or three streams.

Since there is no folding criterion, it is not possible to calculate the parameters of a transition from sheet to stream flow and the changeover between topologically different regimes. Therefore, it is of primary importance to determine experimentally the parametric limits of the existence of such regimes and to detect new ones.

If a metal disk is placed in a water-filled bath, it will sink. What happens if a jet of water from a tap is directed onto this disk (Fig. 14)? One would expect the pressure from the jet to cause the disk to sink even faster. However, this disk does not sink? It floats under the action of the buoyancy force [77, 78]. The clue to the solution of this paradox is that atmospheric pressure acts on the upper surface of the disk, since only a thin stream of water passes along this surface. However, the lower surface is acted upon by the hydrostatic pressure, which his higher than the atmospheric pressure because the disk is immersed in water to a considerably depth. The difference between them creates the buoyancy force, similar to the Archimedean force. The same difference between the pressures is responsible for a characteristic hydraulic water crest (a bora-like effect) near the disk edge. The solution of the problem of such a floating plate has not been obtained in the plane or axisymmetric configurations. It is not clear how important is the role of the viscosity near the edge where a contact discontinuity is formed.

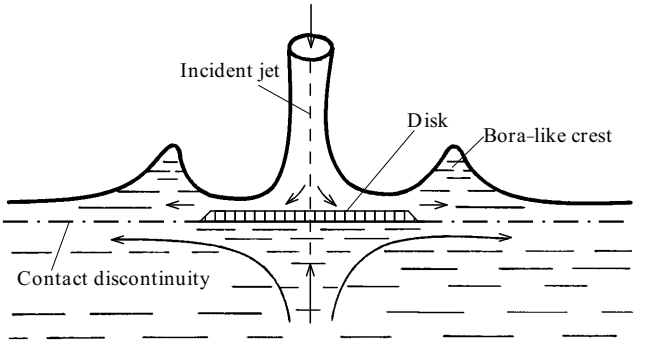

Figure 14. Incidence of a water jet on a floating disk.

The dynamics of air bubbles in water has not been studied at all. One of the surprising phenomena in hydrodynamics is asymmetric flow of water around an air bubble whose typical dimension l is so small that the surface tension forces are important [6, 79]. Such a bubble, propelled by the buoyancy force, follows an upward helical path. The origin of the lateral force which appears in this case is assumed to be not so much the asymmetry of separation of the flow from the air bubble, as periodic oscillations in the nearby wake.

The simplest experiment with a bubble floating upwards involves placing a controlled amount of air, whose volume has a characteristic length l, at the bottom of a water-filled sufficiently high and wide glass vessel. If the value of l is

varied and the other parameters are kept constant, the results give one-parameter dependences of the shape of the bubble, of the coefficients representing the aerodynamic forces acting on the bubble, and of the ratio h/r on the number Re, where h is the pitch of the helical path followed by the bubble and r is the radius of this path.

The shape of the bubble can be calculated on the assumption that the flow is inviscid, symmetric, and nonseparated, that the air pressure inside the bubble is negligible, and that the pressure on its surface is

$$p = \text{const} - \frac{\alpha}{R} ,$$

where α is the surface tension and R is the radius of curvature of the bubble surface. However, even if the solution to this problem does exist, it is of no practical use because the flow past a bubble moving along a helical path is separated.

The simplest outflow problem is that of the shape of a free boundary at the contact between the finite mass of a fluid which is flowing down to the vertex of a cone or a wedge at a rate obeying, for example, a power-law function of time. Does the self-similar regime appear? Which of the factors — viscosity, weight, or capillarity — dominates the final stage of flow? The problem may be converted to one-dimensional form if it is assumed that the vertex angle of the cone or wedge is a small parameter.

4.4 Combined vortices

A three-dimensional vortex of finite size is called *simple* if it has no tangential discontinuities and *combined* if there are such discontinuities. The boundary of a combined vortex is a slip surface: a contact discontinuity, or a free surface. An example of a combined vortex, bounded by a contact discontinuity, is the Hill spherical vortex and an example of a combined vortex bounded by a free surface is the combined Rankine vortex [80].

A combined vortex of finite size is called *hollow* if there is no three-dimensional vorticity, i.e. if $\nabla \times \boldsymbol{u} = 0$, except for the surfaces of a tangential velocity discontinuity. If there is no motion inside such a hollow vortex, then its boundary is a free surface. An example of a hollow vortex, bounded by a vortex sheet, is a planar circular vortex with a point vortex of strength $-\Gamma/2$ located at its centre; here, Γ is the global circulation of the vortex sheet.

The wonderful world of combined vortices has not been investigated at all. It has been found that the interaction of two simple planar vortices is accompanied by the formation of a cusp point and of a vortex sheet [59]. Such an effect (artefact?) has to be reproduced and thoughtfully analysed. No studies have been made of the dynamics of peaking of a tangential discontinuity [81] or of spontaneous (without external forces) appearance of helicity on its smooth surface.

We have considered already a bubble in gradient fluid flow (Fig. 12f). A completely different situation occurs when a thin bubble is in a fluid flowing in the absence of a gradient at a constant velocity u_∞. A pressure gradient is induced by the bubble itself, i.e.

$$p(x, y_1) = p_\infty + \varepsilon p_1(x, y_1) + o(\varepsilon) , \qquad p_\infty = \text{const} .$$

The pressures outside the bubble is found by solving the linear problem of potential flow past a thin body whose shape is given by the expression $y_1 = \varepsilon f(x)$. This pressure is

$$p_1(x, 0) = \frac{\rho u_\infty^2}{\pi} \int_0^l \frac{f'(\xi)}{\xi - x} \, \mathrm{d}\xi .$$

The bubble can 'withstand' this pressure if the velocity inside it, described by the Bernoulli law, is of the order of $\sqrt{\varepsilon}$. Inside the bubble we then have

$$\psi(xP, y_1) = \varepsilon^{3/2} \psi_0(x, y) + o(\varepsilon^{3/2}) , \quad p_1\Big|_{y=f} = -\frac{1}{8} \rho \omega^2 f^2 ,$$

$$\psi_0(x, y) = \frac{1}{2} \omega y (f - y) , \qquad \omega = \text{const} , \qquad y_1 = \varepsilon y .$$

The quality of the pressures outside and inside the bubble together with the action of the surface tension can be described by the following nonlinear integrodifferential equation for the function $f(x)$:

$$\frac{u_\infty^2}{\pi} \int_0^l \frac{f'(\xi)}{\xi - x} \, \mathrm{d}\xi + \frac{1}{8} \omega^2 f^2 - \frac{\alpha}{\rho} f'' = 0 , \tag{4.4}$$

where α is the surface tension. It seems that there are no solutions for $\alpha = 0$.

Formulation of the problem of a bubble in supersonic flow is too exotic for proper treatment. In accordance with the linear supersonic theory, the pressure is proportional to the angle of tilt of the bubble surface or, more exactly,

$$p_1(x, 0) = \rho u_\infty^2 f'(x) .$$

Eqn (4.4) is now replaced with the following ordinary differential equation:

$$u_\infty^2 f' + \frac{1}{8} \omega^2 f^2 - \frac{\alpha}{\rho} f'' = 0 .$$

It is necessary to confirm that the problem of a vortex bubble is well-posed within the framework of the Navier–Stokes equation.

A combined vortex can have a spiral structure. The equation for the transport of the vorticity ω, derived in terms of a system of polar coordinates r and θ is

$$\frac{\partial \omega}{\partial t} + u \frac{\partial \omega}{\partial r} + \frac{v}{r} \frac{\partial \omega}{\partial \theta} = 0 , \tag{4.5}$$

where the stream function is

$$\psi(r, \theta, t) = \frac{1}{4\pi} \int \omega(r^0, \theta^0, t) \times \ln\left[r^2 - 2rr^0 \cos(\theta - \theta^0) + r^{02}\right] r^0 \, \mathrm{d}r^0 \, \mathrm{d}\theta^0 ,$$

$$ru = \frac{\partial \psi}{\partial \theta} , \qquad v = -\frac{\partial \psi}{\partial r} ,$$

and this equation has an exact solution with separable variables:

$$\psi = r^2 \Psi(\eta, t) , \qquad \omega = \omega(\eta, t) ,$$

$$p = r^2 P(\eta, t) , \qquad \eta = \theta + k \ln r .$$

The system of coordinates is nonorthogonal in a physical plane and consists of a family of spirals and a family of circles; the solution is sought in a half-strip defined by $t > 0$, $0 \leqslant \eta \leqslant 2\pi$.

Numerical solution of Eqn (4.5) requires specifying the initial vortex $\omega(\eta, 0)$ and the boundary conditions. The latter conditions can be the equality of the pressures and of

the normal components of the velocity u_n on the $\eta = 0$ and $\eta = 2\pi$ lines, which coincide in a physical plane:

$$P(0, t) = P(2\pi, t), \quad u_n(0, t) = u_n(2\pi, t) .$$

Since the boundary conditions include the pressure, the problem should be supplemented by an equation for determination of $P(\eta, t)$.

Two physically distinct formulations are possible and they are given below.

(1) *Simple vortex*. In this case the tangential components of the velocity remain continuous:

$$u_\tau(0, t) = u_\tau(2\pi, t) .$$

(2) *Combined vortex*. A spiral characterised by $\eta = 0$ (or $\eta = 2\pi$) is a vortex sheet. Since fluid does not cross this sheet, the normal component of the velocity on the sheet is equal to the velocity of the discontinuity $c(t)$:

$$u_n(0, t) = c(t) .$$

There is no certainty that this solution describes 'pseudorandom flow'. However, in analysis of the special case of a self-similar solution [82] spontaneous appearance of an infinite singularity in the distribution of the vortex has been confidently predicted [33]. This phenomenon has been discussed so far for three dimensional flow [84] or for plane vortex sheets evolving in potential flow [85].

4.5 Coordinate expansions in the vicinity of folds

A local solution near a fold, obtained on the basis of the 'dry water' model, is a coordinate series in powers of the distance from the fold. Such a series expansion represents the upper limit of the solution of the problem of the small-scale structure of flow of a low-viscosity fluid. In terms of spherical coordinates r, θ, λ, the solution of the Laplace equation for the velocity potential is sought in the form $r^n f_n(\theta, \lambda) + o(r^n)$. In addition to regular harmonics, which correspond to integral values of n, there are also eigensolutions with fractional values of n. The aim is to find the eigensolution with the smallest index n.

Let us now consider some examples.

The 'three-halves law' (Fig. 15a) for the shape of a vortex sheet near a sharp edge from which this sheet originates [86] breaks down near the edges of a wing. Fig. 15b shows the shape of a wing in plan view. Points A, B, and C are the kinks of the wing profile. Different flow patterns are obtained, depending on the angle of attack (the angle of tilt of a wing relative to the direction of free-stream flow) and on the vertex angle θ at a kink. The nonseparated flow pattern in considered in Ref. [87], but for some reason this is done only for the case when $\theta < \pi$. Linearised solutions have been published [88] and patterns proposed in Ref. [14] have to be checked.

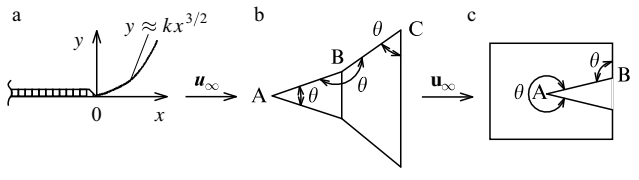

Figure 15. (a) 'Three-halves law'. (b) Kinks in the wing profile (plan). (c) Wing with a longitudinal cut.

Fig. 15c shows the shape of a wing in plan view when the wing has a longitudinal cut. Patterns of flow near folds A and B proposed in Ref. [14] also need to be checked.

There is a greater variety of patterns involving separation from a smooth surface of a body. Topological classification of such patterns should be based on the type of lines of contact of a vortex sheet with the body. Possible cases of three- dimensional separation are shown in Fig. 16: (a) smooth separation; (b) open separation; (c) dipole separation; (d) spiral separation. The three-halves law is valid in sections perpendicular to the line of contact (dashed lines in Fig. 16) and the shape resulting from smooth separation is similar to that obtained for the planar case.

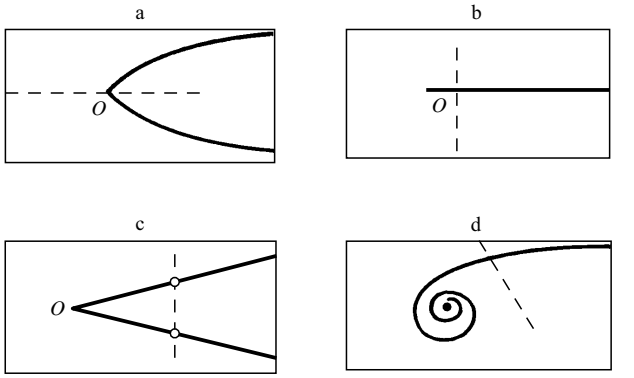

Figure 16. Possible types of lines of contact of vortex sheets with a body.

A coordinate expansion in the vicinity of a vertex line of contact between a vortex sheet and a body has not yet been obtained even for a single case. The problem of a contact discontinuity subject to the surface tension forces has not been tackled: a coordinate expansion has not been obtained even for planar flow; the three-halves law is not valid in the case of separation from a sharp edge or from a smooth surface. Closed vortical regions apparently form in the vicinity of a point of separation, as established experimentally [19].

One of the best known examples of the flow of a compressible fluid for which a coordinate expansion is not known near a fold is the problem of a triple shock proposed by Richtmyer [65] and representing a simple Mach reflection of a shock wave from a wedge. The flow pattern is shown in Fig. 17a, where a contact discontinuity starting from a triple point is represented by a dashed curve and the continuous curves represent self-similar paths. It would seem that the lines of discontinuity should be analytic curves everywhere with the exception of the triple point itself and that the self-similar solutions should be analytic in terms of the variables x/t and y/t. Richtmyer obtained a local solution with the aid of a fractional-exponent series and logarithms. The series derived for each of the angular subregions *1*, *2*, *3*, *4* (Fig. 17a) and satisfying differential equations are matched along the lines of discontinuity. Unfortunately, a solution cannot be obtained in this way. The nature of the singularity still remains unknown. What is the problem? Apparently Richtmyer ignored the special transonic nature of flow near the triple point.

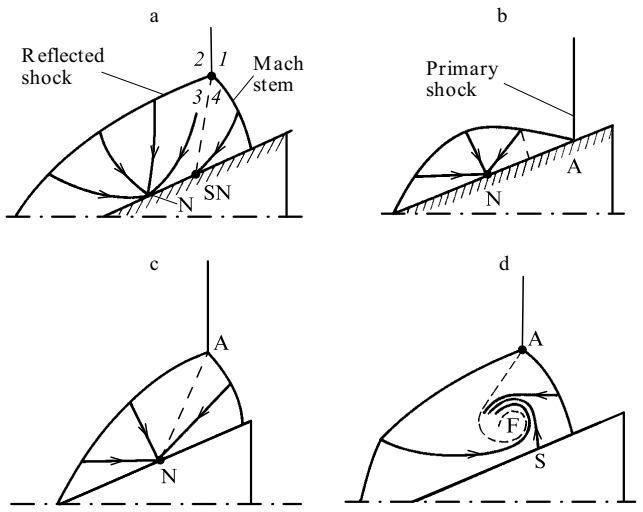

Figure 17. Patterns of reflection of a shock wave from a wedge.

Before we propose a possible explanation of the unsuccessful attempt made by Richtmyer, let us recall that (as established in Section 3) singular points in the field of self-similar paths are located in the region of elliptic equations. For example, under regular reflection conditions the line of parabolicity (dashed line in Fig. 17b) separates 'supersonic' flow in the vicinity of point A from 'subsonic' flow surrounding a node of self-similar paths N.

It is very likely that in the case of simple Mach reflection a line of parabolicity divides an angular region (*4* in Fig. 17a) between a Mach stem and a contact discontinuity into two corner subregions for which the expansions of the solutions are fundamentally different. The ellipticity of the system of equations is important right up to the limiting characteristic.

Similar considerations apply in the case of a steady simple Mach reflection of a shock wave from a solid wall.

Richtmyer's attempt is related also to the following two unsolved problems. One of them, discussed long ago [89], can be solved after the topology of flow has been determined and checked numerically. This is the problem of determination of the criterion of a transition from regular to simple Mach reflection.

The second problem is the behaviour of the end of a contact discontinuity. Fig. 17a applies only if the velocity of a fluid to the left of the contact discontinuity is not equal to the velocity of a point of the saddle + node (SN) type where a slip line is attached to a wedge. It is naturally understood that such a 'separation' pattern is not self-consistent with separation of a self-similar boundary layer from a wedge. Equally doubtful is the simplest topology with just one node N (Fig. 17c) when the velocity of a fluid to the left of a contact discontinuity is equal to the velocity of the point N, i.e. the velocity discontinuity vanishes at this end of a slip line. Under some conditions, experiments reveal the end of a contact discontinuity rolled up into a spiral. Such a flow pattern, which includes a focus and a saddle S (Fig. 17d), is formally self-consistent.

I shall end this subsection by comments which should finally shatter any illusions that we might have about the ease of constructing expansions in the vicinity of folds. A local solution does not always have the simple form of a coordinate series. An alternative case is that when the vicinity of a point (or a line on a surface) has to be split into several (three, ten, or more) subregions and in each of them the initial complete problem has to be simplified. The solutions for such embedded, like the Russian matryoshka toys, subregions are asymptotically compact and mutually correlated. This method had been used first to tackle the problem of flow near a point of separation of a boundary layer in a supersonic stream: this was done by Neiland [90] and also by Stewartson and Williams [91]. Nowadays such expansions are regarded as conventional tools by investigators and the range of their applications is particularly great in the hydrodynamic stability theory, which is an extensive topic we have hardly touched so far.

It follows that a theory of local solutions has not yet been developed not only for the Navier–Stokes equation, but even for the Euler equation.

4.6 Vortex filaments

A vortex filament, which is a mathematical representation of the vorticity concentrated on a line in the delta-function manner, is of little use in modelling real hydrodynamic processes primarily because the velocity and deformation of the filament are generally infinite [6, 92].

Curvilinear vortex filaments are often used in qualitative analysis. Two ring vortex filaments with a common axis should pass through each other periodically. This is mentioned in practically every textbook on hydrodynamics. In experiments it is found that vortex rings are usually ejected through a circular opening as a result of pulsed compression of a closed volume of air. The vortices breaking away from sharp edges of the opening can easily be made visible with smoke.

Under suitable conditions two vortex rings, ejected one after another, merge into one which at first oscillates assuming an elliptic shape and then separates into two new rings. The related paradox, which still has to be resolved satisfactorily, is that during their short interaction these vortices exchange their vorticities. In fact, if initially these rings are coloured differently, then each of the new rings formed as a result of their interaction is coloured half with one colour and the other half with the other colour.

If you carry out this experiment, try to eject several (up to ten) vortex rings following one another at short intervals. The rings will travel some distance along their shared axis and then they will effectively diverge forming a beautiful 'bouquet'. This phenomenon demonstrates the unity of the randomness and regularity principles in the motion of vortices, which is not yet possible to model mathematically.

Can vortex rings pass through one another many times? Maxworthy [93] tried to simulate leap-frogging of vortex rings in water. When the initial velocities of the vortices were approximately the same, two rings merged into one which did not separate later. When the velocity of the second vortex was much higher than that of the first, an unstable composite ring was formed and it then separated into two. As a result, the second ring overtook the first, but then the velocities of the two rings became approximately equal. Therefore, subsequent merging was not observed.

If Maxworthy is correct, then the leap-frogging of vortex rings in water is impossible. Double interaction of vortex rings in air was detected by Yamada and Matsui six years later [19].

Rectilinear vortex lines, moving at a finite velocity, are more suitable for modelling than are curvilinear lines. In

1913, Foppl proposed a pattern for flow past a cylinder, characterised by two symmetrically arranged vortices. These vortices may form not only behind a cylinder but also in front of it [94]. The circulation Γ of these vortices proves to be a free parameter.

In contrast to the Nikol'skii flow, the Foppl model is incorrect: the appearance and existence of point vortices in a real viscous liquid is impossible. However, from the practical point of view this model is very attractive since it predicts zero resistance force. This immediately leads to an interesting idea of deliberate formation of point vortices in the Foppl flow by two rotating cylinders of sufficiently small radius in order to reduce the drag and suppress the wake. An estimate of the energy losses expected in such an experiment shows that it is feasible, but technological difficulties prevent implementation of this idea. We note parenthetically that a rotating cylinder on the surface of a wing profile is being used to move further the point of separation along the wing set at an angle of attack [95].

The Foppl model has another and purely theoretical use: it can be employed to detect unusual properties of separated flow and to carry them over to realistic mathematical models.

The presence of a free parameter Γ in the Foppl model makes it possible to use this model for fluid flow past bodies with sharp edges: the value of Γ can be selected so that the Kutta condition is satisfied or, in other words, the point of separation on a wing is fixed.

Let us consider symmetric flow past a plate with a sharp corner at the origin of the coordinate system (V plate). Let us denote the angles that the plate makes with the x axis by $\pm\alpha\pi$ (Fig. 18a). Let us assume that point vortices of strengths $-\Gamma$ and Γ are located at points z_1 and $\bar{z}_1$. The conformal transformation

$$z = b(\zeta+1)^{1-\alpha}(\zeta-1)^{\alpha}, \qquad b = \frac{1}{2}\,\frac{h}{1-\alpha}\left(\frac{1-\alpha}{\alpha}\right)^{\alpha}$$

maps the exterior of the plate in the z plane onto the ζ plane, in which a section of the axis of abscissae has been removed. The complex-conjugate velocity of flow is

$$\frac{\mathrm{d}w}{\mathrm{d}z} = \frac{\mathrm{d}\zeta}{\mathrm{d}z}\left(bu_\infty - \frac{\Gamma}{2\pi\mathrm{i}}\,\frac{1}{\zeta-\zeta_1} + \frac{\Gamma}{2\pi\mathrm{i}}\,\frac{1}{\zeta-\bar{\zeta}_1}\right).$$

If under steady conditions (no external force) we go to the limit

$$\lim_{z\to z_1}\left(\frac{\mathrm{d}w}{\mathrm{d}z} + \frac{\Gamma}{2\pi\mathrm{i}}\,\frac{1}{z-z_1}\right) = 0\,,$$

we find that two algebraic equations are obtained:

$$(\xi_1-k)(\xi_1^2-\eta_1^2-1) = 2\xi_1\eta_1^2\,,$$

$$\left(1-\frac{2\eta_1}{g}\right)(3\xi_1^2-\eta_1^2-2k\xi_1-1) = 1-k^2\,,$$

where $2\pi u_\infty a g = \Gamma$, $k = 1-2\alpha$, $\zeta_1 = \xi_1 + \mathrm{i}\eta_1$.

The Kutta condition at the sharp edge

$$\frac{\mathrm{d}w(k)}{\mathrm{d}\zeta} = 0$$

completes the problem of determination of ξ_1, η_1, and g by the third algebraic equation:

$$(k-\xi_1)^2 + \eta_1^2 = 2g\eta_1\,.$$

The geometric locus of the centre of vortices is plotted as a function of α in Fig. 18a. At low values of α (or in the limit $\alpha \to 1$) a weak point vortex is located in the vicinity of the edge. As α increases to 0.5, which corresponds to flow past the plate, the vortex strength increases without limit and the vortex escapes to infinity along asymptotes which make the angle $\pm\pi/6$ with the abscissa. Thus, contrary to the currently held ideas [94], there is no solution to the problem of symmetric flow past the plate characterised by two point vortices. This is the essence of the Foppl paradox. In a broader sense the work, the Foppl paradox can be used to denote the absence of a steady solution of a problem for certain critical values of the determining parameters σ_{cr} if vortices are removed to infinity by going to the limit $\sigma \to \sigma_{\mathrm{cr}}$.

Does bifurcation in the asymmetric Foppl flow pattern occur at $\alpha = 0.5$? Does the Foppl paradox apply to other configurations or to other distributions of the vorticity, apart from those concentrated at points? It is interesting to note that the solution of the problem of flow past such a V plate does exist in the Nikol'skii scheme for any value of α.

Can the Foppl model be applied to flow inside a wedge-shaped region? The problem is that the flow of a strongly viscous liquid ($Re \to 0$) is characterised by an infinite chain of three-dimensional vortices of decreasing alternating-sign strength, located in a wedge-shaped region (Fig. 18b). This chain has been observed experimentally and is known under the name of Moffatt vortices [19, 96]. Such a system of vortices is an exact solution of the Stokes equation. A similar solution of the Navier–Stokes or Euler equations is not known.

One of the possible solutions of the Euler equation is a sequence of point vortices with the circulation Γ_m, located at points x_m on the bisector of a wedge. The condition for the

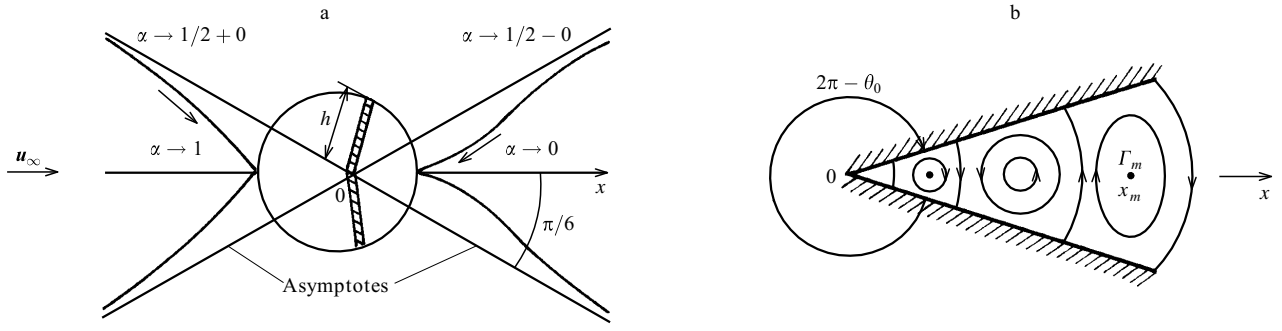

Figure 18. Two problems with point vortices.

absence of a force acting on each point vortex leads to an infinite system of transcendental equations:

$$\sum_{j\neq m} \frac{\Gamma_j \xi_j}{\xi_m^2 - \xi_j^2} = \frac{2\theta_0 - \pi}{4\pi} \frac{\Gamma_m}{\xi_m} ,$$

where $\xi_m = x_m^{\pi/2\theta_0}$ and θ_0 is the wedge angle. The simple solution $\Gamma_m = (-1)^m$, $x_m = m = 1, 2, 3, \ldots$ exists only when $\theta_0 = \pi$.

Systems of point vortices evolving in the absence of solid boundaries are being investigated intensively. An example is what is known as a *discrete-circular vortex* (Fig. 19), which is a symmetric system of point vortices located on N concentric circles in such a way that the same number of k vortices with the same circulation is located on each circle.

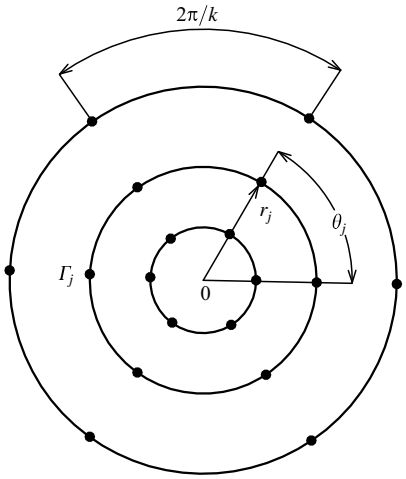

Figure 19. Discrete-circular vortex.

One general comment should be made on the stability of symmetric clusters: it relates to the methods of investigating this stability. We can study symmetry breaking in a system as a whole on the assumption that its components are stable entities and, having determined the symmetry as the exact solution of the problem, we can then study instability of an individual component. This division of the problem into two parts opens up possibly the only way for investigating the stability of symmetric vortex structures.

In the case of a discrete-circular vortex we can study the behaviour of all the kN vortices. It is found that a 'cloud' of vortices exhibits a symmetry instability [86] similar to the Helmholtz instability of a contact discontinuity [69], whereas a discrete-circular vortex breaks down immediately. In the other case we can select one vortex on each circle and having determined the symmetry positions of the other vortices, we can study instability of N vortices. The mechanism of this instability is not known, but it is fundamentally different from the Helmholtz instability.

Thus, if on each circle we select one vortex with the circulation $T_j (j = 1, 2, \ldots, N)$ and with the complex coordinate

$$z_j(t) = r_j(t) \exp\left[\mathrm{i}\theta_j(t)\right] ,$$

we find that the functions $r_j(t)$ and $\theta_j(t)$ obey a system of $2N$ ordinary differential equations. The Kirchhoff invariants are retained [6].

In the course of motion a sign of the quantity $r_{j+1} - r_j$ may change. If $N = 2$, this resembles the leap-frogging of vortices discussed above. It occurs when initially r_1/r_2 is less than a certain critical value of σ. It is of interest to consider the dependence of σ on Γ_2/Γ_1, which represents the boundary of the region where such a vortex leap-frogging takes place. This is useful in determination of the discretisation step in numerical calculations of multispiral vortex sheets.

If $N = 2$, flow is deterministic, but for $N > 2$, we can expect chaos. One of the probable scenarios of the appearance of chaos is the formation of an ε layer on the separatrices in the phase space [97].

It is not known whether collapse of a discrete-circular vortex is possible. This problem is closely related to the problem of stability of conventional collapse of three point vortices† discussed above because, in the limit $t \to 0$ ($t = 0$ is the collapse time), the main contribution comes from the selected three collapsing vortices and the remaining $k - 1$ vortex triplets have only a correction that decreases with time.

As pointed out above, chaos in a system of point vortices does occur when their number exceeds three. This conclusion applies to the evolution of vortices in unbounded space. Are the properties of a system of three point vortices the same in bounded space? Here, the term 'bounded space' means either an internal region (wedge, circle) or a region external relative to the body around which fluid flows. The simplest problem is that of the evolution of three point vortices above an impermeable plane, which is equivalent to three symmetric (relative to this plane) pairs of point vortices in infinite space.

Can chaos occur in the case of evolution of a discrete-circular vortex, located inside or outside a circle, if $N = 2$?

Point vortices provide good opportunities for modelling both small and large perturbations in the dynamics of an ideal incompressible fluid. Such perturbations frequently not only deform, but also destroy coherent entities. The problem is formulated as follows: at $t = 0$, point vortices are introduced into a moving fluid and these begin to interact with one another and with solid boundaries. Depending on the previous history of flow and on the nature of this interaction, three variants are possible: there is no separation, vortices initiate separation which has not occurred earlier at $t < 0$, and vortices interact with a well-advanced separation, which exists when $t < 0$, and is — for example — in the form of free boundaries. Specific problems are considered in Ref. [14].

5. Rotational flow

Rotational flow refers to three-dimensional motion with a specific fluid rotation axis. Even in the 'dry water' approximation it is found that fast rotational motion has surprising properties: change of equation from elliptic to hyperbolic, formation of Proudman–Taylor columns, proportionality of the drag of a body not to the acceleration, but to the velocity or ... the path (!) travelled by a body [6, 99, 100]. However, the general theory of rotational laminar flow is still far from complete.

†The problems of existence and stability of steady and uniformly rotating point-vortex clusters is discussed in Ref. [98].

5.1 Flow past bodies

Axisymmetric flow of an ideal incompressible fluid can be described by the following parameters: the modulus of the maximum angular velocity Ω, the characteristic dimension l of the body past which the fluid is flowing, the axial velocity u_∞ which is constant far from this body. Then, the influence of rotational flow can be described by the Rossby number

$$Ro = \frac{u_\infty}{\Omega l} .$$

The Euler equation is then [6]

$$\psi_{xx} + \psi_{rr} - \frac{1}{r}\psi_r = Ro^{-2}\left[r^2 H'(\psi) - C(\psi)C'(\psi)\right] ,$$

where the various quantities are made dimensionless as follows: the stream function ψ is divided by $u_\infty l^2$, the cylindrical coordinates x and r are divided by l, the total pressure H in a stream line is divided by $pl^2\Omega^2$, and the velocity of circulation around the symmetry axis ($r = 0$) is divided by $l^2\Omega$; the functions $H(\psi)$ and $C(\psi)$ are specified by the conditions at infinity ($x = -\infty$), where $\psi = r^2/2$.

If $Ro \ll 1$ the overall flow is independent of x and the stream function is found from

$$r^2 H' = CC' . \tag{5.1}$$

A change occurs only in a thin inviscid boundary layer of thickness $O(Ro)$ adjoining the surface of the body. In the simplest case of flow past a disk (Fig. 20a) the stream function ψ_0 in the boundary layer is found from the equation

$$\frac{\partial^2\psi_0(\xi, r)}{\partial\xi^2} = r^2 H'(\psi_0) - C(\psi_0)C'(\psi_0)$$

with the boundary conditions (5.1) in the limit $\xi \to \pm\infty$ and subject to the condition $\psi_0 = 0$ when $\xi = 0$, where $x = \xi Ro$.

If $\Omega = \infty$, then $Ro = u_\infty l/\Gamma$, where Γ is the circulation of a vortex filament. The problem of uniform flow of a fluid represented by a vortex filament ($r = 0$) in the Helmholtz scheme has not yet been solved (Fig. 20b).

A very different problem is represented by the case when flow turns under the action of a rotating body and there is no rotation at infinity. A mathematical model of the Proudman–Taylor columns, which then appear ahead of a body and behind it (Fig. 20c), has not yet been developed. It is also worth noting the disappearance of a rear column on reduction in the Reynolds number $Re = u_\infty l/\nu$. The Proudman–Taylor columns in an ideal fluid extend along the x axis to $\pm\infty$ (dashed lines in Fig. 20c).

If the axial velocity u is divided by u_∞, the radial v and circular w velocities are divided by Ωl, and the pressure is divided by $\rho(\Omega l)^2$, the Navier–Stokes equations become

$$\begin{aligned}
&Ro\,\frac{\partial u}{\partial x} + \frac{1}{r}\frac{\partial(rv)}{\partial r} = 0 ,\\
&Ro\,u\,\frac{\partial v}{\partial x} + v\,\frac{\partial v}{\partial r} - \frac{w^2}{r} = -\frac{\partial p}{\partial r} + \alpha\left(\nabla^2 v - \frac{v}{r^2}\right) ,\\
&Ro\,u\,\frac{\partial w}{\partial x} + v\,\frac{\partial w}{\partial r} + \frac{vw}{r} = \alpha\left(\nabla^2 w - \frac{w}{r^2}\right) ,\\
&Ro\,u\,\frac{\partial u}{\partial x} + v\,\frac{\partial u}{\partial r} = -\frac{1}{Ro}\,\frac{\partial p}{\partial x} + \nabla^2 u ,
\end{aligned} \tag{5.2}$$

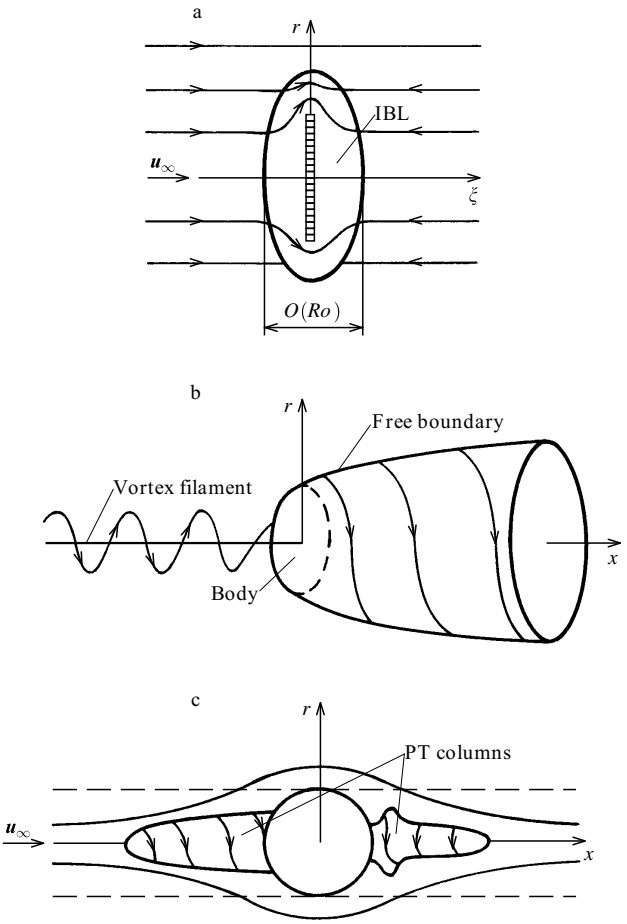

Figure 20. (a) Inviscid boundary layer (IBL) on a disk. (b) Interaction of a vortex filament with a body in the Helmholtz model. (c) Proudman–Taylor (PT) columns.

were

$$\alpha Re = Ro , \qquad \nabla^2 = \frac{\partial}{\partial x^2} + \frac{1}{r}\frac{\partial}{\partial r}\left(r\,\frac{\partial}{\partial r}\right) .$$

The next two nonlinear submodels correspond to the cases of strongly rotating ($Ro \ll 1$) and weakly rotating ($Ro \gg 1$) fluids.

(1) $Ro \ll 1$. A body is flattened along the x axis and its shape is described by the equation $x = Rof(r)$. The pressure is independent of ξ an and the dependence $p(r)$ is found from the conditions at infinity ($\xi \to -\infty$):

$$\frac{dp}{dr} = \frac{w^2}{r} , \qquad u = 1 , \qquad v = 0 .$$

The reduced Navier–Stokes equations follow from the system of equations (5.2):

$$\begin{aligned}
&\frac{\partial u}{\partial \xi} + \frac{1}{r}\frac{\partial(rv)}{\partial r} = 0 ,\\
&u\,\frac{\partial v}{\partial \xi} + v\,\frac{\partial v}{\partial r} - \frac{w^2}{r} = -\frac{dp}{dr} + \alpha\,\frac{\partial^2 v}{\partial \xi^2} ,\\
&u\,\frac{\partial w}{\partial \xi} + v\,\frac{\partial w}{\partial r} + \frac{vw}{r} = \alpha\,\frac{\partial^2 w}{\partial \xi^2} .
\end{aligned}$$

(2) $Ro \gg 1$. A theory of a thin body now applies and the equation for the surface is $r = Ro^{-1}f(x)$. The pressure is

found separately from the second equation by the Navier – Stokes equations converted to the parabolic form:

$$\frac{\partial u}{\partial x}+\frac{1}{\eta}\frac{\partial(\eta v)}{\partial \eta}=0\ ,$$

$$u\frac{\partial w}{\partial x}+v\frac{\partial w}{\partial \eta}+\frac{vw}{\eta}=\beta\left[\frac{1}{\eta}\frac{\partial}{\partial \eta}\left(\eta\frac{\partial w}{\partial \eta}\right)-\frac{w}{\eta^2}\right]\ ,$$

$$u\frac{\partial u}{\partial x}+v\frac{\partial u}{\partial \eta}=\beta\left[\frac{1}{\eta}\frac{\partial}{\partial \eta}\left(\eta\frac{\partial u}{\partial \eta}\right)-\frac{u}{\eta^2}\right]\ ,$$

where $\eta = rRo$, and $\beta Re = Ro^2$.

A numerical calculation begins at the point $x=-1$. There are singular regions near the front and rear edges.

It is usual to distinguish the 'entry point' of flow (Fig. 21a) and the 'exit point' (Fig. 21b). Within the framework of the Euler equations, these two types of flow are indidstinguishable because of the principle of reversibility of flow. In the vortex-free case a rectilinear vortex filament, located on the continuation of the axis of a cone, starts from the vertex A of this cone. In fact, the conditions of axial symmetry, written down for the potential φ in a spherical system of coordinates r, θ, and λ

$$\frac{\partial^2\varphi}{\partial r\,\partial\lambda}=\frac{\partial^2\varphi}{\partial\theta\,\partial\lambda}=0\ ,$$

determines directly the form of its function:

$$\varphi(r,\theta,\lambda)=\varphi_1(r,\theta)+\varphi_2(\lambda)\ .$$

It follows from the Laplace equation $\nabla^2\varphi=0$ that $2\pi\varphi_2(\lambda)=\Gamma\lambda$, where Γ is a constant. Therefore, the continuation of the attached vortex filament AB is a free filament AC with the circulation Γ (Fig. 21). Such a local solution implies dependence on time as a parameter.

In view of linearity of the problem, the loss of the axial symmetry can be investigated separately. If the potential is represented by a Fourier series

$$\varphi(r,\theta,\lambda)=\sum_{k=1}^{\infty}\Phi_k(r,\theta)\sin(k\lambda)$$

and the solution for low values of r is limited to a power law

$$\Phi_k(r,\theta)=r^nF_k(\theta)\ ,$$

the Laplace equation leads to the Legendre equation for F_k. The condition of zero flow on the cone $[F_k'(\theta_0)=0]$ and the 'Kutta condition' of a finite velocity on the axis $\theta=0$ $[F_k(0)=0]$ complete the formulation of the $n(k)$ *eigenvalue problem*.

A vortex filament is extremely unstable. A slight deformation of a part of the filament causes it to move, theoretically, at infinite velocity. Therefore, the pattern of flow with a vortex filament can hardly serve as an external expansion for the solution obtained for the problem of flow of a viscous liquid when $Re=\Gamma/\nu\to\infty$, where ν is the kinematic viscosity. The self-similar solution proposed for the $\theta_0=\pi/2$ case in Ref. [101] is unacceptable because it ignores diffusion of a vortex filament and it does not exist for sufficiently large values of the number Re.

The mechanism of appearance of rotational flow can be made more specific on the assumption that the investigated cone rotates uniformly about its axis. Then the solution of the local problem should be sought in the half-strip $r\geqslant 0$, $0\leqslant\theta\leqslant\theta_0$ subject to the condition of zero velocity on the $\theta=\theta_0$ line and the minimal singularity conditions on the lines $\theta=0$ and $r=0$. A soliton solution of this problem $(\theta_0=\pi/2)$ was obtained by von Karman (see, for example, Ref. [102]).

5.2 Self-rotation of bodies in flow

If a body is hinged at a point or a shaft, it has the freedom to rotate in a flowing fluid. Rotation of a body which is not damped out with time is called self-rotation. The energy of such rotation is drawn from the flow outside the body. Experiments have shown that steady, oscillatory, and disordered self-rotation is possible.

The published investigations have been concerned mainly with self-rotation about the axis coinciding with the direction of free-stream flow.

Self-rotation of a rectangular plate was discovered by Zhukovskii in 1906. This rotation took place in a range of attack angles corresponding to a negative derivative (with respect to the angle of attack) of the normal force [103]. Only then an aerodynamic torque rotating a wing is observed.

Self-rotation of an ellipsoid with the aspect ratio of 5 about an axis coinciding with its minor axis and with the direction of free-stream flow is surprising: in the case of such a body the flow past it is independent of the angle of attack and there is no lift force [104]. An increase in the Reynolds number Re first does not alter the frequency of rotation (?) and then $(Re=Re_{cr})$ in the ellipsoid stops and begins to rotate $(Re>Re_{cr})$ in the opposite direction (mystically?) at a higher angular velocity. Self-rotation is explained by the asymmetry of Hertler vortices on the upstream and downstream parts of the ellipsoid. An experiment of this kind must be repeated and analysed.

Self-rotation is of practical importance for manoeuvrable aircraft. Such aircraft have low-aspect-ratio wings $(\lambda\ll 1)$ and, therefore, the centre of interest has shifted to studies of their rotation [105]. The topic of first importance is then the interaction of the vortices trailing off from both side edges, their evolution, and breakup. Mathematical modelling of the majority of these effects is possible on the assumption that the fluid is ideal. In particular, it is necessary to develop the

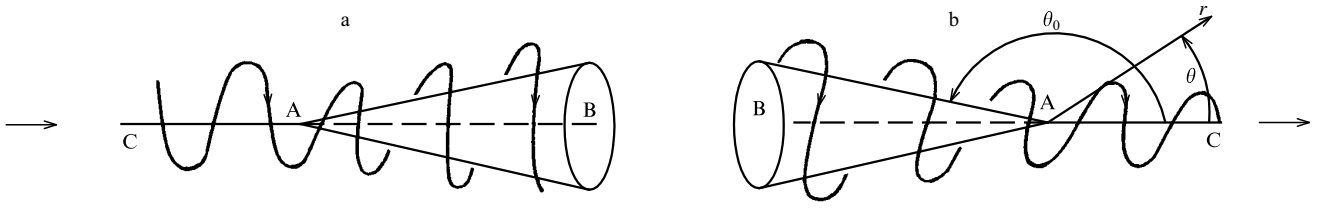

Figure 21. Interaction of a vortex filament with a cone: (a) 'entry point'; (b) 'exit point'.

law of planar cross section for a rotatable low-aspect-ratio wing.

Conversely, in aerodynamics of self-rotating wingless rockets the viscosity effects are of prime importance: separation of a boundary layer on a rotating wall and laminar–turbulent transition [106].

Even a slight asymmetry can greatly enhance self-rotation. This effect is observed if a hole is made in a solid sphere placed in an air stream.

Self-rotation patterns of double configurations are surprising and varied [107]. Two cylinders, whose axes are parallel to one another but perpendicular to the direction of free-stream flow, can self-rotate. A child's rattle, which is a configuration of several spheres hinged to a ring, also self-rotates.

5.3 Channel flow

A typical problem of internal flow of a fluid can be solved if the solution is not based on the Navier–Stokes equation but, for example, on its parabolised subanalogue. One of such mathematical models is discussed below.

Let a fluid travel between two concentric cylinders (Fig. 22). The flow is turned by rotation of the inner cylinder at a velocity δw_1 and of the outer cylinder at a velocity δw_2; here, δ is a dimensionless parameter such that $\delta = O(1)$ or $\delta = o(1)$. The width of the annular channel between the cylinders is small: the outer cylinder has the radius $(1+\varepsilon)r_0$, where r_0 is the radius of the inner cylinder and $\varepsilon \ll 1$. The dimensionless form of the coordinate x is obtained if we divide it by r_0, and instead of r use a stretched variable

$$R = \frac{r - r_0}{\varepsilon r_0}, \quad 0 \leqslant R \leqslant 1 .$$

The case can be made more general by assuming that the fluid is injected or drawn off at a characteristic velocity τu_∞ along the normal to the surface of both cylinders; here, u_∞ is the characteristic velocity of axial motion and $\tau = O(\varepsilon)$ or $\tau = o(\varepsilon)$.

Substitution of the expansions of the velocity components

$$u = \frac{\tau}{\varepsilon} U(x, R) + o\left(\frac{\tau}{\varepsilon}\right), \quad v = \frac{\tau u_\infty}{\Omega l} V(x, R) + o(\tau) ,$$

$$w = \frac{\delta w_1}{\Omega l} W(x, R) + o(\delta)$$

into the system of equations (5.2) yields the following expressions which are obtained from the first and third equations:

$$UW_x + VW_R = \frac{1}{Re} W_{RR}, \quad U_x + V_R = 0 ,$$

where $Re = \tau\varepsilon u_\infty r_0/\nu = O(1)$.

The conditions which apply on the cylinder surfaces

$$\begin{aligned} &U(x, 0) = U(x, 1) = 0, \quad V(x, 0) = V_1(x) , \\ &V(x, 1) = V_2(x), \quad W(x, 0) = 1, \quad W(x, ,) = \frac{w_2}{w_1} \end{aligned} \tag{5.3}$$

contain the functions $V_1(x)$ and $V_2(x)$, which are assumed to be given.

Estimates of the pressure are contradictory. It follows from the second equation of the system (5.2) that

$$p = O(\varepsilon\delta^2) + O(\tau^2) ,$$

but the third equation gives

$$p = O\left(\frac{\tau^2}{\varepsilon^2}\right) .$$

Depending on the relationships between $\varepsilon\delta^2$ and τ^2/ε^2, we can distinguish the following three cases.

(1) Strong rotation:

$$\varepsilon^3\delta^2 \gg \tau^2, \quad p = \varepsilon\delta^2\rho w_1^2 P(x, R) + O(\varepsilon\delta^2) .$$

The solution is obtained in a closed form:

$$\frac{\partial P}{\partial x} = 0, \quad \frac{\mathrm{d}P(R)}{\mathrm{d}R} = W^2, \ldots .$$

(2) Weak rotation

$$\varepsilon^3\delta^2 \ll \tau^2, \quad p = \frac{\tau^2}{\varepsilon^2}\rho w_1^2 P(x, R) + o\left(\frac{\tau^2}{\varepsilon^2}\right) .$$

The boundary layer approximation can be used:

$$P_R = 0, U_x + V_R = 0, UU_x + VU_R = -P'(x) + \frac{1}{Re} U_{RR} .$$

(3) Basic model:

$$\varepsilon^3\delta^2 = \tau^2, \quad p = \varepsilon\delta^2\rho w_1^2 P(x, R) + o(\varepsilon\delta^2) .$$

The system of equations

$$\begin{aligned} &U_x + V_R = 0, \quad P_R = W^2 , \\ &UW_x + VW_R = \frac{1}{Re} W_{RR} , \\ &UU_x + VU_R = -P_x + \frac{1}{Re} U_{RR} \end{aligned} \tag{5.4}$$

is compatible with the boundary conditions (5.3). Moreover, it is necessary to specify the initial values of the functions in a certain section $x = 0$: $U(0, R)$, $V(0, R)$,

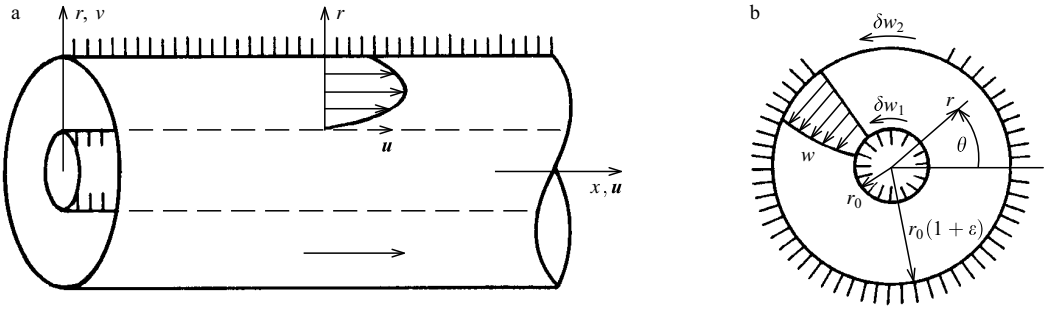

Figure 22. Channel flow pattern.

$W(0, R)$, and $P(0, R)$. In this initial set there are two interdependent functions:

$$P_R = W^2 ,$$

$$2VWW_R - VUU_{RR} + U^2 V_{RR} = \frac{1}{Re}(2WW_{RR} - UU_{RR}) .$$

In a numerical calculation one can use the Crank–Nicholson scheme or an implicit three-layer scheme [3–4].

If $Re = 0$, the solution is in quadratures:

$$U = Re\, A'(x)\,\frac{R(R-1)}{2} , \qquad Re\, A''(x) = 12(V_2 - V_1) ,$$

$$V = V_1 + (V_1 - V_2)R^2(2R - 3) ,$$

$$W = 1 + R\left(\frac{w_2}{w_1} - 1\right) , \qquad P = \int W^2\, dR + A(x) .$$

It is of interest to consider to stability of the solution of the system of equation (5.4).

The well-known problem of steady axisymmetric outflow of water from a bath under the action of the force of gravity has not yet been solved. The model of an ideal fluid is applicable provided

$$Re = \frac{\sqrt{gd^3}}{\nu} \gg 1 ,$$

where g is the acceleration due to gravity and d is the diameter of the drain hole. The problem is governed by a single dimensionless parameter $\sigma = h/d$, where h is the undisturbed level of water.

It is known from experience that in a certain range of values of σ $(\sigma_1 < \sigma < \sigma_2)$ the flow begins to rotate spontaneously. Is there only one value of the angular velocity Ω of the stream? Is Ω the eigenvalue of the problem or is it found from the considerations of stability? Is the method of boundary integral equations applicable to this problem?

The experimentally observed increase in the rate of flow of water when it is rotating can obviously be explained by an increase in the thickness of the stream under the action of centrifugal forces.

The problem of an axisymmetric fountain can also be extended to the case of rotation of water around the x axis (Fig. 23). The initial distribution of the vertical velocity $u(r)$ is fairly arbitrary. Is separation of sheets and formation of bubbles possible? A thin-stream approximation is discussed in Ref. [108].

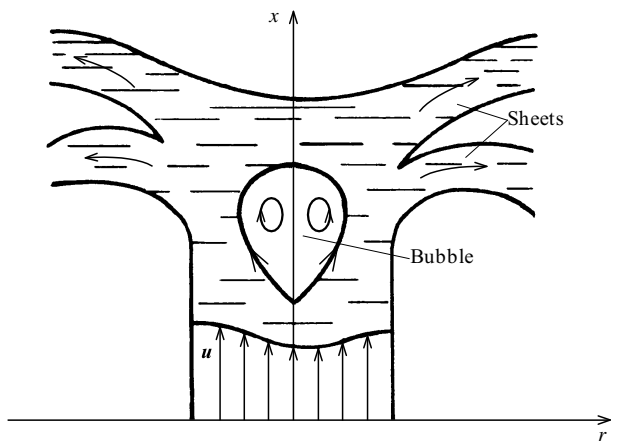

Figure 23. Axisymmetric fountain.

5.4 Once again about spiral flow

Spiral motion is a special case of rotational flow. In describing spacial spiral vortex structures, I found to my chagrin that I do not know the mathematical definition of the spiral even as a planar curve. I found that this is not a simple matter! I cannot accept as this definition the following abracadabra statement given in *Matematicheskii Entsiklopedicheskii Slovar'* (Encyclopedic Mathematical Dictionary) published by Sovetskaya Entsiklopediya (Moscow 1988): "The spiral is a planar curve, which usually (?—my query) passes around one (or several) points, approaching or moving away from it." This unmathematical definition fits also, for example, an ellipse.

In fluid dynamics the spiral is usually (!) understood to be a curve with an infinite number of turns. Therefore, I shall define a spiral as a planar curve which makes an infinite number of rotations as it reels in on a simple closed curve or on a point. In the first case the simple closed curve is called the *limit cycle*.

In mathematical models the number of turns of a spiral is infinite, but our experience shows that the number of turns is finite: the nature, as pointed out already, does not tolerate infinities.

A *spiral surface* is a surface which has a simple curve as its axis. The surface is such that its normal section is a spiral with the focus located on the axis. It follows that the axis of a spiral surface is a focal curve, which is the geometric locus of the foci of the spirals. The axis of a cylindrical spiral surface is a straight line and the spirals are the same in each section.

A *spatial spiral line* is the path of a particle moving along a spiral surface in such a way that a spiral is obtained by projection onto a plane normal to the axis. A *screw (helical) line* is a spatial line describing the path of a particle which rotates about a certain straight line (axis) and at the same time moves parallel to this line.

In the modelling of spatial spiral flow it is convenient to use coordinate systems with an axis and an azimuthal angle λ. These are, for example, spherical (r, θ, λ) and cylindrical (x, r, λ) coordinates. Instead of λ, a spiral variable $\eta = \lambda + g$ is used; here $g = g(r, \theta, t)$ in a spherical system of coordinates and $g = g(x, r, \lambda)$ in a cylindrical one. The conditions of spiral periodicity mentioned earlier apply for $\eta = 0$ and $\eta = 2\pi$.

The shape of a waterspout-like vortex sheet in the plane of symmetry of flow and also near a smooth surface where sheet begins has not been investigated. Are steady self-similar solutions applicable in this case?

Spiral flow occurs over rotating bodies or in rotating containers. No studies have been made of bifurcation of axisymmetric flow to spiral flow. Is there an analogue of the Hill vortex [6] in slowly rotating spiral flow?

The self-similar steady solution of the Navier–Stokes equation in a spherical system of coordinates is

$$\boldsymbol{u}(r, \theta, \lambda) = \frac{\nu}{r}\boldsymbol{U}(\theta, \eta) , \qquad p(r, \theta, \lambda) = \frac{\nu^2}{r^2}P(\theta, \eta) ,$$

$$g(\theta, r) = k \ln r + f(\theta) .$$

The region where the solution exists is bounded by the rectangle $0 \leqslant \eta \leqslant 2\pi$, $0 \leqslant \theta \leqslant \pi$. In the special case of axisymmetric flow $(\partial/\partial\eta = 0)$ with $(w \not\equiv 0)$ or without $(w \equiv 0)$ rotation the equation can be reduced to the ordinary form and the spiral periodicity conditions are

unnecessary. Three formulations of this problem are known: axisymmetric flux of momentum from a point source, flow induced by a vortex filament located along the axis of a cone, and flow induced by a linear source also located on the cone axis. All these three formulations need to be extended to the case of spiral flow.

Axisymmetric flow can be generalised conveniently to this case by adopting a cylindrical system of coordinates. Interesting approximations are those of rapidly convergent ($(r|\partial g/\partial r| \gg 1$) and slowly convergent ($r|\partial g/\partial r| \ll 1$) spirals. Can the limit cycle appear in the field of streamlines?

Although it has long been known that a waterspout has a spiral structure, only axisymmetric models have been investigated. Such a formulation is suitable only for the modelling of a waterspout-like vortex which breaks off from the surface of a wing. A real waterspout can be modelled only if the compressibility, the force of gravity, and heat conduction are taken into account.

The exact self-similar solution

$$u_x = \frac{vx}{r^2}\,u(\eta)\,, \qquad u_r = \frac{v}{r}\,v(\eta)\,, \qquad u_\lambda = \frac{v}{r}\,w(\eta)\,,$$

$$p = \frac{v^2}{r^2}\,P(\eta)\,, \qquad \eta = \lambda + k\ln r$$

describes spiral flow in the symmetry plane $x = 0$. It can be treated as a truncated coordinate expansion in powers of x of a non-self-similar solution in the vicinity of the symmetry plane $x = 0$.

The planar Hamel flow, described by the stream function $\psi = \psi(\eta)$, where $\eta = \lambda + k\ln r$, as well as its various generalisations [42, 109] are not physically realisable since they do not satisfy the spiral periodicity conditions.

It is not known whether a spiral boundary layer builds up on a rotating body in a stream and, in particular, whether this happens on a rotating disk.

6. Hydrodynamics in a bath

Experiments in a bath are mentioned frequently in the preceding section, but no reference has been made to the well-known experiments of Magnus, Rank, Taylor, Marangoni, Toms, and others [9, 110]. However, even a superficial examination of any of these experiments reveals unsolved problems and incompleteness of the conventional interpretation.

Let us consider, for example, the experiment with tea leaves. Why do they gather at the centre of the bottom of a glass after the tea has been stirred with a spoon? The answer to this question was published by Einstein himself: tea leaves are driven to the centre by flow at the bottom of the glass. Although no rigorous calculations of the motion of tea leaves has been made, there is evidence that the 'wet' tea leaves at the bottom of the glass of density exceeding that of water rotate not at the centre of the glass but near it and form a 'belt of asteroids'. The width of this 'belt' depends on the degree of inhomogeneity of the tea leaves: leaves of different sizes and masses rotate along circles of different radii. They collect at the centre only during the final stage of their deceleration.

We perform these 'experiments' on tea leaves daily, but we do not pay proper attention to their behaviour. It would be necessary to determine how not only the 'wet' tea leaves, but the also 'dry' leaves (i.e. those that float in the interior and on the surface of water) behave during motion and its final stage. Instead of tea leaves, we can consider other particles and it is desirable that they should be of calibrated size. In addition to mixing with a spoon, we can use a 'purer' method of rotational motion: we can rotate a glass of tea by clamping it in a mixer or placing it at the centre of a rotating disk in a record player. We can make the following experiments with tea leaves: (a) determine their positions during rotation or after; (2) rotate tea or glass; (3) observe bottom, surface, floating leaves. This is a total of $2 \times 2 \times 3 = 12$ combinations. However, this is not all! We can exclude the influence of deformation of the free surface by, for example, covering tightly the water in the glass with a cover. We can also do other things. the reader can think of other ways of carrying these apparently simple but really extremely complex experiments.

It is hardly likely that Einstein expected the concentration of tea leaves at the centre of a glass to find an application in technology. However, this effect has been used in a centrifuge designed for industrial purification of tin: molten metal rotates in this centrifuge, impurities are collected at the centre, and removed automatically.

Scientific experiment differs from contemplation in that it is designed for the development, checking, or improvement of the mathematical model of the investigated phenomenon.

6.1 Evolution of a free surface

True 'experiments in a bath' involve a free surface.

In hydrodynamics of capillary liquids there is an unanswered fundamental question of the time taken by a meniscus to rise in a cylindrical tube. Is this time finite or infinite? The inertial term is ignored in Ref. [111]. Therefore the law of motion of a meniscus obtained there is exponential and the time taken by the meniscus to approach equilibrium is infinite. In fact, the inertial term is of the same order of magnitude as the other terms: it cannot be neglected. It has been shown [14] that the exponential law is valid only in the case of a highly viscous liquid and that the column of a low-viscosity liquid will oscillate about an equilibrium position. These conclusions need to be checked experimentally.

A liquid film remains on the surface of a solid taken out from a liquid. If the solid is a plate, drawn upwards parallel to itself (Fig. 24a), the liquid becomes entrained under the action of tangential (i.e. viscosity) forces. Flow can be regarded as steady if the dimensions of the vessel and the length of the plate are sufficiently large (Fig. 24b) and the plate is pulled out at a constant velocity u_0. The dimensional determining parameters u_0, v, g, ρ and the surface tension α can be used to form two dimensionless combinations:

$$Re = \frac{u_0^3}{gv} \quad \text{and} \quad We = \frac{\rho u_0^4}{g\alpha}\,.$$

There are two characteristic scales in this case: the length $l_{\text{visc}} = v/u_0$, governed by the viscosity forces, and the length $l_{\text{cap}} = (\alpha/\rho g)^{1/2}$, governed by the capillary forces. Their ratio is

$$\frac{l_{\text{cap}}}{l_{\text{visc}}} = \frac{Re}{\sqrt{We}}\,.$$

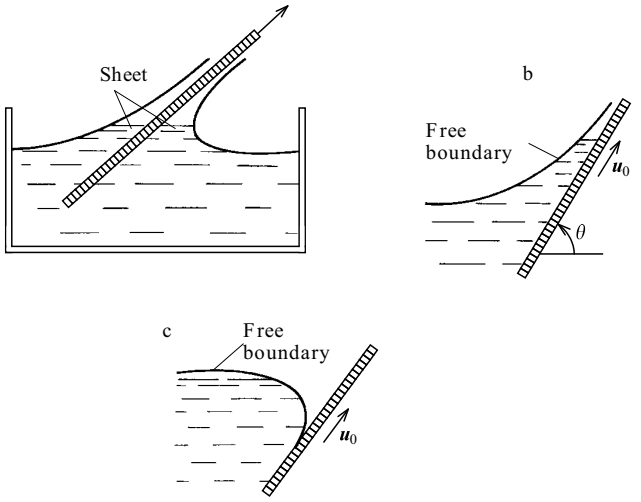

Figure 24. Formation of a sheet on a plate drawn out of water.

Depending on the order of magnitude of the ratio of the Reynolds Re and Weber We numbers ($\gg 1$, ~ 1, $\ll 1$), there are $3 \times 3 = 9$ asymptotic flow submodels†, which have to be checked experimentally. The structure of the film extracted with the plate is described by an internal expansion obtained in the thin-layer approximation.

One can formulate the problem of immersion of a plate in a wetting liquid. In the corresponding problem of pulling out of a plate there is a critical value of the number $Re(We, \theta)$ which distinguishes the regime when the entrained film wets the whole of the plate from the regime when such a film does not form (Fig. 24c).

It is of interest to consider unsteady and in particular self-similar problems of a plate entering a half-plane of liquid at rest and a plate leaving such a liquid.

6.2 Sprays and splashes

A splash represents ejection (usually upwards) of water in the form of a jet or a sheet. Sprays are liquid droplets which scatter rapidly after an impact or a splash. Can you recall the Russian poet Alexander Pushkin: ''People were herded, admiring splashes, mountains, and foam of enraged waters''?

Waterfalls, breaking waves, impact of waves on a rock, and collisions of meteorites with solid surfaces are all accompanied by splashes. The relevant unsolved problems are collected in Ref. [112], but the one-dimensional mathematical model of a splash used there does not stand up even to a mildly critical examination. It is not clear whether the Moore–Rott–Sirs splash criterion for the detachment of a boundary layer is satisfied.

Splashes usually break up into sprays. The spray-formation mechanisms are various. For example, a liquid jet may break up into droplets under the influence of turbulence, Rayleigh instability, or capillary instability [19]. Large masses of a liquid (over 100 g) break up into sprays because they cannot be held together by the surface tension forces. This fact reduces significantly the efficiency of fire fighting by large masses of water dropped from aircraft. After the answer has been found how the surface tension and the method by which water is ejected affect spray formation, the problem should be subject to a 'brainstorming' attack by inventors.

†The model proposed in Ref. [111] is phenomenological and not asymptotic.

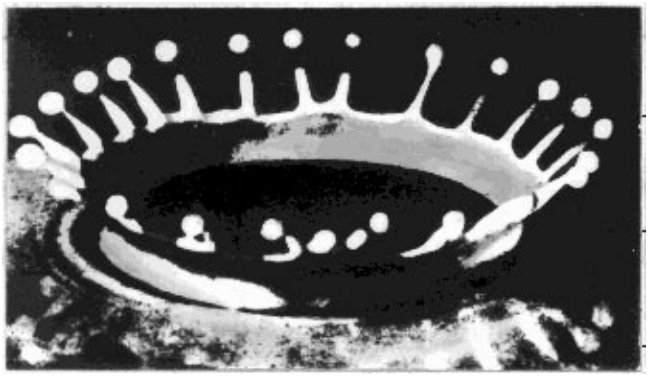

Figure 25. Impact of a milk drop on a flat surface.

A splash in the form of an opposite jet called the 'sultan' is formed when a drop is incident on a free surface of a liquid. A drop falling on a solid surface produces very different effects. The whole world has seen photographs of a splash consisting of 24 sprays distributed symmetrically on a circle (Fig. 25) [107]. Such a 'coronet' forms when a drop of milk hits a solid surface. The drop strikes the plane surface and spreads into a patch. Waves with a period $360^\circ/24 = 15^\circ$ along the angular coordinate form at the boundary of this patch. The milk becomes detached from the plane it struck and the separated thin layer splits into 24 sprays. This was the moment at which a photograph was taken. The motion then becomes chaotic. Why precisely 24 sprays are formed? What is the influence of the viscosity and surface tension forces? There is as yet no answer to this and other questions.

Experimental investigations of the fragmentation of a liquid droplet began at the dawn of aviation (1904). Such investigations are of great scientific and technological importance. Applications include chemical processes in two-phase media, drying of sprays, erosion of turbine blades, formation of aerosols, operation of gas turbines and of diesel and rocket engines, and combustion chambers with liquid injection.

Six types of fragmentation of an initially spherical liquid droplet in a gas stream are known [113]: vibrational, bag type, stamen-like, chaotic, stripping type, and catastrophic. The main parameters which determine the fragmentation processes are

$$\frac{\rho}{\rho_0}\,,\quad Re = \frac{u_\infty d}{\nu}\,,\quad \frac{\nu}{\nu_0}\,,\quad We = \frac{\rho u_\infty^2 d}{\alpha}\,,\quad M_\infty = \frac{u_\infty}{a}\,,$$

where ρ is the density of the liquid, ρ_0 is the density of the gas in which fragmentation takes place, ν is the kinematic viscosity of the liquid, ν_0 is the kinematic viscosity of the gas, u_∞ is the flow velocity, d is the initial diameter of the droplet, α is the surface tension, and a is the velocity of sound in the gas.

An attempt to construct, on the basis of the available experimental data, in a $Re-We$ diagram the limits of the various types of fragmentation of a water droplet in slowly ($M_\infty \approx 0$) moving air has proved to be internally inconsistent. It is not clear whether the fault lies in the insufficient precision of the experiments or whether the problem in hand has some hidden determining parameter on which the fragmentation mechanism depends.

6.3 Boundary waves

If a plate is immersed vertically in a water-filled bath to a small depth (about 4 mm) and if this plate is made to vibrate in a horizontal plane, unusual 'boundary' waves are observed. This is what the discoverer of these waves, Michael Faraday, founder of electromagnetism, had to say: ''Immediately waves, protuberances, and folds of very unusual kind began to form in water. Waves propagating from the plate to the walls of the vessel were almost unnoticeable while whole swellings of a height from one-third to one-half inch and more were incessantly appearing near the plate perpendicularly to it; they were alike very short teeth of a coarse comb''. The frequency of these waves was equal to half the frequency of the plate vibrations [107, 114].

Two kinds of boundary waves should be distinguished. The existence of waves of one type, which form near a vibrating sharp edge of a plate, is due to flow separation from the edge.

The second type of boundary waves is observed when there is no separation from the sharp edge. They appear, for example, in a water-filled glass if its edge is rubbed carefully with a wet finger and vibrations of the glass are thus excited. Nothing is known about the nature of these waves, observed by the inquisitive Faraday.

References

1. Prigogine I, Stengers I *Order out of Chaos: Man's New Dialogue with Nature* (New York: Bantam Books, 1984)
2. Babenko K I *Osnovy Chislennogo Analiza* (Fundamentals of Numerical Analysis) (Moscow: Nauka, 1986)
3. Fletcher C A *Computational Techniques for Fluid Dynamics* 2 vols (Berlin: Springer, 1988)
4. Anderson D A, Tannehill J, Pletcher R *Computational Fluid Mechanics and Heat Transfer* (New York: Hemisphere Publications, 1984)
5. Alfven H ''Cosmology and physics'', translated into Russian in *Nauka i Chelovechestvo. 1970–1972* (Science and Humanity, 1971–1972) (Moscow: Znanie, 1972) p. 332
6. Batchelor G K *An Introduction to Fluid Dynamics* (Cambridge: Cambridge University Press, 1967)
7. Heywood J C *Lect. Notes Math.* **1431** 1 (1990)
8. Ginzburg V L *O Fizike i Astrofizike* (On Physics and Astrophysics) (Moscow: Nauka, 1985)
9. Burlaki N *Kvant* (2) 42 (1992)
10. Kolmogorov A N *Matematika — Nauka i Professiya* (Mathematics — Science and Profession) (Moscow: Nauka, 1988) [*Kvant Library*, No. 64]
11. Kapitza P L *Eksperiment. Teoriya. Praktika* (Experiment. Theory. Practice) (Moscow: Nauka, 1977)
12. Lavrent'ev M A *Nauka i Zhizn'* (7) 9 (1965); (1) 48 (1966)
13. *Sakharovskii Sbornik* (Sakharov Collection, compiled by A Babenyshev, R Lert, E Pechuro) (Moscow: Kniga, 1991)
14. Betyaev S K, Preprints TsAGI Nos 26, 36, 48, 55, 58, 64, 71, 72, 85, 97 (Zhukovski, Moscow Province: Central Aerohydrodynamic Institute, 1991–1994)
15. Ursell F, in *Asymptotic Methods in Wave Mechanics* (Eds G Wickham, P A Martin) (Cambridge: Cambridge University Press, 1992)
16. Burlaki N, Preprint TsAGI No. 73 (Zhukovski, Moscow Province: Central Aerohydrodynamic Institute, 1993)
17. Zakharov V E, Sagdeev R Z, Khalatnikov I M, Preprint (Chernogolovka, Moscow Province: Landau Institute of Theoretical Physics, 1985)
18. Gould H, Tobochnik J *Introduction to Computer Simulation. Applications to Physical Systems*, Parts 1 and 2 (Reading, MA: Addison-Wesley, 1988)
19. Van Dyke M (Ed.) *An Album of Fluid Motion* (Stanford, CA: Parabolic Press, 1982)
20. Andrews J G, McLone R R (Eds) *Mathematical Modelling* (London: Butterworths, 1976)
21. Zaslavskii G M, et al. *Slabyi Khaos i Kvaziregulyarnye Struktury* (Weak Chaos and Quasiregular Structures) (Moscow: Nauka, 1991)
22. Betyaev S K, Preprint ITPM No. 14-93 (Novosibirsk: Institute of Theoretical and Applied Mechanics, Siberian Division of the Academy of Sciences of the USSR, 1983)
23. Bulakh B M *Nelineinye Konicheskie Techeniya Gaza* (Nonlinear Conical Flow of a Gas) (Moscow: Nauka, 1970)
24. Edwards R H *J. Aeronaut. Sci.* **21** (2) 134 (1954)
25. Smith J H B *Proc. R. Soc. London Ser. A* **306** 67 (1968)
26. Massau *Memoire sur l'integration graphique des equations aux derivees partielles* (Delporte: Mons., 1914)
27. Rosenhead L *Proc. R. Soc. London Ser. A* **134** 170 (1931)
28. Westwater F L *Aero. Res. Council Rep. Mem.* (1692) 116 (1936)
29. Kaden H *Ing. Arch.* (2) 140 (1931)
30. Fermi E, Pasta D, Ulam S, in *Enrico Fermi: Scientific Works* [translated into Russian] (Moscow: Nauka, 1972), Vol. 2
31. Sedov L I *Metody Podobiya i Razmernosti v Mekhanike* (Similarity and Dimensional Methods in Mechanics) (Moscow: Nauka, 1977)
32. Zel'dovich Ya B, Raizer Yu P *Physics of Shock Waves and High Temperature Hydrodynamic Phenomena* 2 vols (New York: Academic Press, 1966–1967)
33. Barenblatt G I *Podobie, Avtomodel'nost', Promezhutochniya Asimptotika* (Similarity, Self-Similarity, Intermediate Asymptotics) (Moscow: Gidrometeoizdat, 1978)
34. Betyaev S K *Zh. Vychisl. Mat. Mat. Fiz.* **26** 1081 (1986)
35. Birkhoff G *Hydrodynamics: A Study in Logic, Fact, and Similitude* (Princeton, NJ: Princeton University Press, 1950; reprinted New York: Dover, 1955)
36. Busemann A, in *Gasdynamik* [translated into Russian] (Moscow: IL, 1950) p. 197 of the Russian translation
37. Nikol'skii A A *Dokl. Akad. Nauk SSSR* **116** 193 (1957)
38. Nikol'skii A A *Dokl. Akad. Nauk SSSR* **116** 365 (1957)
39. Nikol'skii A A, Betyaev S K, Malyshev I P, in *Problemy Prikladnoi Matematiki i Mekhaniki* (Problems in Applied Mathematics and Mechanics) (Moscow: Nauka, 1971) p. 262
40. Aref H *Phys. Fluids* **22** 393 (1979)
41. Lamb H *Hydrodynamics* 6th edition (New York: Dover, 1945)
42. Kochin N E, Kibel' I A, Roze N V *Teoreticheskaya Gidrodinamika* (Theoretical Hydrodynamics) (Moscow: Fizmatgiz, 1963) Part 2
43. Betyaev S K *Dokl. Akad. Nauk SSSR* **257** 1310 (1981) [*Sov. Phys. Dokl.* **26** 359 (1981)]
44. Betyaev S K *Tr. Tsentr. Aerogidrodinam. Inst.* (2275) (1985)
45. Betyaev S K *Uch. Zap. Tsentr. Aerogidrodinam. Inst.* **1** (3) 15 (1970)
46. Tugazakov R Ya *Izv. Akad. Nauk SSSR Mekh. Zhidk. Gaza* **24** (2) 159 (1989)
47. Betyaev S K, Solntsev I A *Prikl. Mat. Mekh.* **48** 145 (1984)
48. Arkhangel'skii N A, Shurshalov L V *Izv. Akad. Nauk SSSR Mekh. Zhidk. Gaza* **12** (1) 83 (1977)
49. Prandtl L, in *VortraSge aus Hydro- und Aerodynamik* (Berlin; Springer, 1924) p. 18
50. Mangler K W, Weber J *J. Fluid Mech.* **30** 177 (1967)
51. Karman T *Ann. Mat. Pura Appl.* **29** (4) 247 (1949)
52. Brown S N, Mangler K W *Aeron. Quart.* (11) 354 (1967)
53. Telionis D P *Unsteady Viscous Flow* (Berlin: Springer, 1981)
54. Betyaev S K *Tr. Tsentr. Aerogidrodinam. Inst.* (2517) (1993)
55. Neiland V Ya *Uch. Zap. Tsentr. Aerogidrodinam. Inst.* **5** (2) 70 (1974)
56. Zababakhin E I, Zababakhin I E *Yavleniya Neogranichennoi Kumulyatsii* (Unlimited Cumulation Phenomena) (Moscow: Nauka, 1988)
57. Potter D E *Computational Physics* (New York: Wiley-Interscience, 1973)
58. Petviashvili V I, in *Nelineinye Volny* (Nonlinear Waves) (Moscow: Nauka, 1979) p. 5

59. Deem G S, Zabusky N J, in *Solitons in Action* (Eds K Lonngren, A Scott) (New York: Academic Press, 1978)
60. Burbea J *Lett. Math. Phys.* (6) 1 (1982)
61. Lavrent'ev M A, Shabat B V *Problemy Gidrodinamiki i Ikh Matematicheskie Modeli* (Problems in Hydrodynamics and Their Mathematical Models) (Moscow: Nauka, 1973)
62. Molchanov V F *Uch. Zap. Tsentr. Aerogidrodinam. Inst.* **6** (4) 1 (1975)
63. Tumashev G G, Muzhin M T *Obratnye Kraevye Zadachi* (Inverse Boundary-Value Problems) (Kazan: Kazan State University, 1965)
64. Giraud J *Fundamental Properties in the Theory of Hypersonic Flow* [translated into Russian] (Moscow: Mir, 1965)
65. Richtmyer R D *Principles of Advanced Mathematical Physics* 2 vols (Berlin: Springer, 1979, 1981)
66. Tikhonov A N, Arsenin V Ya *Metody Resheniya Nekorrektnykh Zadach* (Methods for Solution of Ill-Posed Problems) (Moscow: Nauka, 1979)
67. Chorin A J, Bernard P S *J. Comput. Phys.* **13** 423 (1973)
68. Fink P T, Soh W K *Proceedings of Tenth Symposium on Naval Hydrodynamics, Cambridge, MA, 1974* p. 463
69. Birkhoff G, in *Hydrodynamic Instability* [translated into Russian] (Moscow: Mir, 1964) p. 68 of the Russian translation
70. Polozhii G N *Obobshchenie Teorii Analiticheskikh Funktsii Kompleksnogo Peremennogo* (Generalisation of the Theory of Analytic Functions of Complex Variables) (Kiev: Kiev State University, 1965)
71. *Istoriya Otechestvennoi Matematiki* (History of Soviet Mathematics) (Kiev: Naukova Dumka, 1970) Vol. 4, Part 1, p. 295
72. Yeung R W *Annu. Rev. Mech.* **14** 395 (1982)
73. Gurevich M I *Teoriya Strui Ideal'noi Zhidkosti* (Theory of Ideal Fluid Jets) (Moscow: Nauka, 1979)
74. Walker J *Nauka Vokrug Nas* (12) 92 (1984)
75. Van Dyke M *Perturbation Methods in Fluid Mechanics* (New York: Academic Press, 1964)
76. Hasimoto H, Sano O *Mechanics: News from Foreign Science—Vortices and Waves* [translated into Russian] (Moscow: Mir, 1984) p. 80 of the Rusian translation
77. Olsson R G, Turkdogan E T *Nature (London)* (211) 813 (1966)
78. Luzin A N *Kvant* (10) 19 (1986)
79. Birkhoff G, Zarantonello E H *Jets, Wakes, and Cavities* (New York: Academic Press, 1957)
80. Milne-Thomson L M *Theoretical Hydrodynamics* 4th edition (London: Macmillan, 1960)
81. Whitham G B *Linear and Nonlinear Waves* (New York: Wiley-Interscience, 1974)
82. Betyaev S K, Gaifullin A M *Izv. Akad. Nauk SSSR Mekh. Zhidk. Gaza* **17** (5) 53 (1982)
83. Saffman P G *J. Fluid Mech.* **106** (1981) [*A Special Issue Celebrating the Twenty-Fifth Anniversary of the Journal* (Eds G K Batchelor, H K Moffatt) (Cambridge: Cambridge University Press, 1981)]
84. Morf R H, Orszag S A, Frisch U *Phys. Rev. Lett.* **44** 572 (1980)
85. Moore D W *Proc. R. Soc. London Ser. A* **365** 105 (1979)
86. Betyaev S K, in *Dinamika Sploshnoi Sredy so Svobodnymi Poverkhnostyami* (Dynamics of a Continuous Medium with Free Surfaces) (Cheboksary: Cheboksary State University, 1980) p. 27
87. Brown S N, Stewartson K *J. Inst. Math. Appl.* **5** 206 (1969)
88. Medan R T, AGARD Report CP-204 No. 18 (1977)
89. Griffiths W *J. Fluid Mech.* **106** (1981) [*A Special Issue Celebrating the Twenty-Fifth Anniversary of the Journal* (Eds G K Batchelor, H K Moffatt) (Cambridge: Cambridge University Press, 1981)
90. Neiland V Ya *Izv. Akad. Nauk SSSR Mekh. Zhidk. Gaza* **4** (4) 53 (1969)
91. Stewartson K, Williams P G *Proc. R. Soc. London Ser. A* **312** (1509) 181 (1969)
92. Widnall S E *Annu. Rev. Fluid Mech.* **7** 141 (1975)
93. Maxworthy T *J. Fluid Mech.* **51** 15 (1972)
94. Villart H *Lecons sur la theorie des tourbillons* (Paris: Gauthier-Villars, 1930)
95. Modi V J, et al. *J. Aircraft* **28** (2) 104 (1991)
96. Moffatt H K *J. Fluid Mech.* **18** 1 (1964)
97. Rabinovich M I, Trubetskov D I *Vvedenie v Teoriyu Kolebanii i Voln* (Introduction to the Theory of Oscillations and Waves) (Moscow: Nauka, 1992)
98. Aref H, et al. *Fluid Dyn. Res.* (3) 63 (1988)
99. Nikol'skii A A *Tr. Tsentr. Aerogidrodinam. Inst.* (2122) (1981)
100. Lugt H *Vortex Flow in Nature and Technology* (New York: Wiley, 1983)
101. Gol'dshtik M A, Shtern V N, Yavorskii N I *Vyazkie Techeniya s Paradoksal'nymi Svoistvami* (Viscous Flow with Paradoxical Properties (Novosibirsk: Nauka, 1989)
102. Landau L D, Lifshitz E M *Fluid Mechanics* 2nd edition (Oxford: Pergamon Press, 1987)
103. Martynov A K *Prikladnaya Aerodinamika* (Applied Aerodynamics) (Moscow: Mashinostroenie, 1972)
104. Korotkin A I *Uch. Zap. Tsentr. Aerogidrodinam. Inst.* **4** (25) 26 (1973)
105. Zee E M, Batina J T *J. Aircraft* **28** (2) 94 (1991)
106. Hemsch M, Nielsen J *Tactical Missile Aerodynamics* (New York: American Institute of Aerodynamics and Aeronautics, 1986)
107. Walker J *The Flying Circus of Physics. With Answers* (New York: Wiley, 1978)
108. Nikulin V V *Zh. Prikl. Mekh. Tekh. Fiz.* (4) 42 (1992)
109. Schultz-Piszachick W *Z. Angew. Math. Mech.* **62** 115 (1982)
110. Betyaev S K *Kvant* (8) 52, (10) 52 (1989)
111. Levich V G *Fiziko-Khimicheskaya Gidrodinamika* (Physico-chemical Hydrodynamics) (Moscow: Fizmatgiz, 1959)
112. Peregrine D H *J. Fluid Mech.* **106** (1981) [*A Special Issue Celebrating The Twenty-Fifth Anniversay of the Journal* (Eds G K Batchelor, H K Moffatt) (Cambridge: Cabridge University Press, 1981)
113. Wierzba A, Takayama K *Rep. Inst. High Speed Mech. Tohoku Univ.* **53** (382) 1 (1987)
114. Walker J *Sci. Am.* **253** (2) 98 (1985)